Chapter 14

Systematic Study of Ethylene-Vinyl Acetate (EVA) in the Manufacturing of Protector Devices for the Orofacial System

Reinaldo Brito e Dias, Neide Pena Coto,
Gilmar Ferreira Batalha and Larissa Driemeier

Additional information is available at the end of the chapter

http://dx.doi.org/10.5772/intechopen.69969

Abstract

Fracture of facial bones and dental elements, and laceration of soft tissue, have increased in sports over recent years. Dentist is the only professional responsible for the mouth protection design, the knowledge about suitable materials is essential. EVA is a thermoplastic material, available in the market, easy of handling and processing, and low-cost. However, it is important to understand the mechanical properties and ability to absorb and to dissipate the impact energy, when this material is submitted to different environments, such as oral cavity with saliva and different temperatures. This chapter show provides a systematic evaluation of the EVA application in orofacial protectors while focusing on sports. The research comprises two aspects: experimental tests and numerical analyses. During experimental tests, EVA was analyzed in special buccal conditions, concerning temperature and presence of saliva. Regarding the presence of saliva, more specific studies about its influence on the mechanical behavior of EVA were performed. In the numerical analyses of the EVA orofacial protector, the studies focused on its effect on the nasal bone integrity, and in the zygomatic bone protection. However, life cycle should be analyzed, since its performance deteriorates over time. Mainly due to the saliva-originated changes to the EVA mechanical characteristics, it can behave as a rigid material. For facial protection, a better performance is obtained with a combination of rigid and soft EVA material. According to the experimental and numerical results from a systematic study of EVA, its application to orofacial protection can be considered satisfactory.

Keywords: material tests, orofacial protection, trauma in sports, protection in sports

1. Introduction

According to the World Health Organization (WHO) [1], "Health is a state of complete physical, mental and social well-being and not merely the absence of disease or infirmity."

Areas of study related to life, health and disease are called human health sciences. Medicine, Biology, Biomedicine, Nursing, Speech Therapy, Pharmacy and Biochemistry, Sports Science, Physical Education, Psychology, Occupational Therapy, Nutrition, Physiotherapy, Bioengineering and Dentistry are part of this program. All these research areas focus on improving or maintaining the patient quality of life, in accordance with the conditions dictated by WHO.

In dentistry, a particularly important area is related to the endless search for materials that can more efficiently help the maintenance and/or return of the individual's well-being. Researchers in dentistry seek and study materials that may replace dental organs, may be accepted in the alveolar and dentofacial complex, or may protect the orofacial complex from injuries.

Therefore, due to the technical-scientific excellence required in its attributions, dentistry is a science that requires constant updating of materials science and applications. It is worth highlighting that, to indicate a safe and efficient clinical application for a particular material, mechanical, physical, chemical and biological properties must be known.

According to Anusavice et al. [2], four groups of materials are used and studied in dentistry: metals, ceramics, composites and polymers. These materials are separated into modalities, according to their application: preventive, restorative or auxiliary materials.

Auxiliary are materials with recognized importance and application but which do not fit into the first two modalities. It is the best option for describing the function of polymers.

Polymers are an important category of materials for dentistry. They are versatile, since they can be combined in order to improve mechanical properties, and moreover, they are reproducible and homogeneous [3].

The term polymer derives from the Greek words: poly-many and mer-unit; or, more specifically, it is a macromolecule composed of repeating units linked by a covalent bond. Its physical properties depend on the length of the molecule and its molar mass. When the polymer is formed by a single type of *mer*, it is called **homopolymer**; otherwise, it is called a **copolymer**.

According to their malleability, polymers are classified into thermoplastic and thermosetting. When the temperature is raised above its melt point, the *thermoplastic polymer* becomes softer and more fluid, allowing it to be molded. When the heat source is removed, the thermoplastic hardens in the molded shape. Since it occurs without chemical curing, it is a reversible physical transformation. In turn, with the addition of a second material and/or heat, *thermosetting polymers* soften and cure, forming cross-links that prevent the material from returning to the primary form. This process cannot be repeated.

http://dx.doi.org/10.5772/intechopen.69969

Regarding mechanical behavior, polymers are classified as *elastomers*, *plastics* and *fibers* [4].

During dentists' day-to-day operations, *resin* is the most commonly used polymer. Most of these resins are based on methacrylate, with methyl methacrylate as the main ingredient. Resins are easy to manipulate, without demanding elaborate techniques; the final resin products are esthetically acceptable and offer excellent balance when used in the oral environment, in the presence of saliva and chewing conditions, besides being low cost [5].

Ethylene-vinyl acetate (EVA), object of this study, is a thermoplastic copolymer derived from petroleum. For dental use, it is in the form of rigid or flexible flat plates, in thicknesses of 1–5 mm, without the presence of blowing agents, differently from EVA plates available in the common market. It is indicated as a shock absorber material, for producing mouth and facial protectors for sports practice, as pointed out by Coto et al. [6], as well as dental bleaching trays, orthodontic restraints and as the base for facial prostheses.

2. Ethylene-vinyl acetate

The copolymer of ethylene and vinyl acetate is a thermoplastic polymer, formed by different monomers: ethylene and vinyl acetate (**Figure 1**). Monomers merge through a polymerization process—a set of reactions among simple molecules to form a macromolecule of high molar mass.

The EVA presents semi-crystalline structure; its geometry is composed of an amorphous and a crystalline part. The damping capacity of EVA increases as the percentage of vinyl acetate decreases. As already mentioned, EVA is a macromolecule composed of repeated units linked by covalent bonds and its primary units of constitution are two monomers whose physical properties depend on their size and molecular weight. Polymeric materials generally exhibit density ranging from 0.926 to 0.950 g/cm^3, temperature resistance (glass transition temperatures

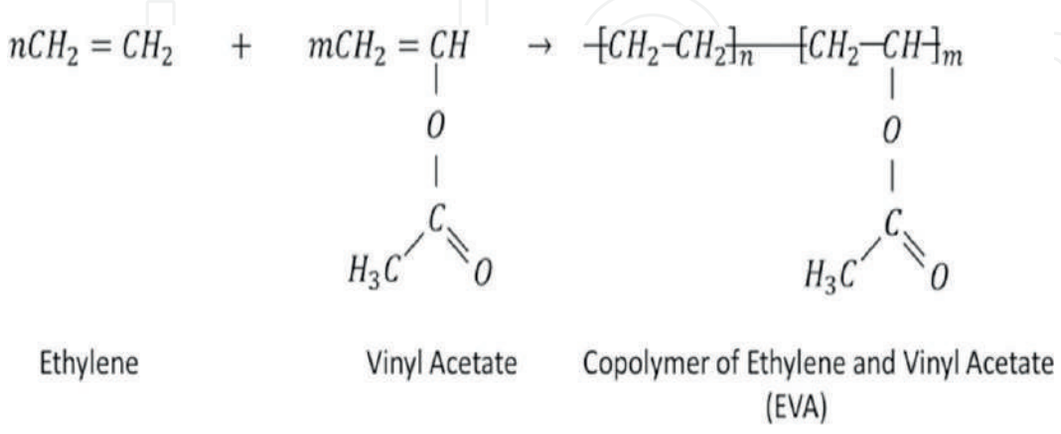

Figure 1. Polymerization reaction between ethylene and vinyl acetate, resulting in EVA.

close to 0 to −7°C). Among the main characteristics of EVA, its elastic behavior characterized by the Young Modulus ranging from 15 to 80 MPa can be highlighted. Flexible EVA, for example, behaves similarly to elastomers, and its elasticity is considerable.

In most practical situations in which EVA is applied or mechanically tested, it is possible to observe that the material's mechanical response is time dependent, that is, it is a viscoelastic material. This characteristic of viscosity is important for energy dissipation.

In the chemical industry, EVA is presented in grain form as shown in **Figure 2**.

Some mechanical properties of EVA are discussed as follows.

2.1. Stiffness

The initial stiffness of the EVA can be measured by its modulus of elasticity, that is, angle of inclination of the approximated straight line that relates stresses as a function of the strains, in elastic regime. In the elastic regime, the energy absorbed by the deformed material is totally restored by removing the stress. The higher the vinyl acetate concentration, the more flexible the EVA material is, due to the reduction in the degree of crystallization.

The degree of EVA crystallization is proportional to the latent heat of fusion (ΔH_f), and its value increases as the concentration of crystals present in EVA increases. However, EVA is not a totally crystalline polymer because, in the solid state, it contains two phases: amorphous and crystalline. In fact, the presence of a glass transition temperature (T_g) means that it contains an amorphous phase, since T_g is a thermal transition exclusive of the amorphous phase, that is, it is the temperature at which the macromolecules of the amorphous phase acquire rotational mobility. The amorphous phase of EVA is represented by a macromolecule entanglement which lacks an ordered and periodic three-dimensional structure. The crystalline phase, on the other hand, is characterized by a three-dimensional ordered and periodic structure of macromolecules folded one on the other, assuming the lamellar format. The melting temperature (T_f) is also a thermal transition, in which the crystalline phase disintegrates and the polymer becomes a viscous liquid.

Figure 2. EVA in granules.

http://dx.doi.org/10.5772/intechopen.69969

2.2. Hardness

The hardness of a polymer is determined by the penetration of the Durometer indenter foot into a small sample (Shore Hardness). The increase in vinyl acetate content reduces the hardness of EVA, mainly due to the decrease in its degree of crystallization. Although hardness and stiffness are different properties, in some cases, it is possible to establish an empirical correlation between them for a given family of polymers. In some cases, as the degree of crystallization of EVA increases, the stiffness and hardness increase proportionally.

2.3. Transparency

The polymer crystals of EVA act as physical obstacles to the passage of light. Accordingly, as the polymer crystals concentration decreases, increasing the content of vinyl acetate, the material becomes more transparent.

2.4. Damping

It is the ability of the material to absorb the mechanical energy to mainly overcome internal friction. The damping capacity of EVA increases as the vinyl acetate content reduces. Damping capacity is sometimes unduly related to hardness. However, a hard polymer can be designed to have the same damping capacity of a soft polymer.

2.5. Viscoelasticity

In many of the practical conditions in which polymers are requested or tested, their mechanical response is found to be time-dependent, which characterizes these materials as viscoelastic, as already mentioned. This absorption may occur due to the internal friction between the macromolecules, by shape changes (rotation of the carbon–carbon bonds around its own axis) or by flow. Furthermore, in case of impact, the viscous portion is responsible, for the delay in the elastic response, which will depend on the stimulus and on the time necessary to coil and to uncoil the polymer macromolecule [4, 7–9].

3. Experimental study of EVA applied to oral protection

The study of the mechanical properties of EVA focused on mouth guards and facial protectors. Particularly for the facial protector designed in this study, a patent was applied (number BR 20 023048 9).

Several experimental tests made with the material, available in the literature [10–12], confirm this percentage, which is proportionally inverse to the EVA damping capacity. Moreover, the EVA was carefully characterized in POLITENO—Brazil (now BRASKEN) for analysis. The analyses of vinyl acetate percentage were performed by means of pyrolysis.

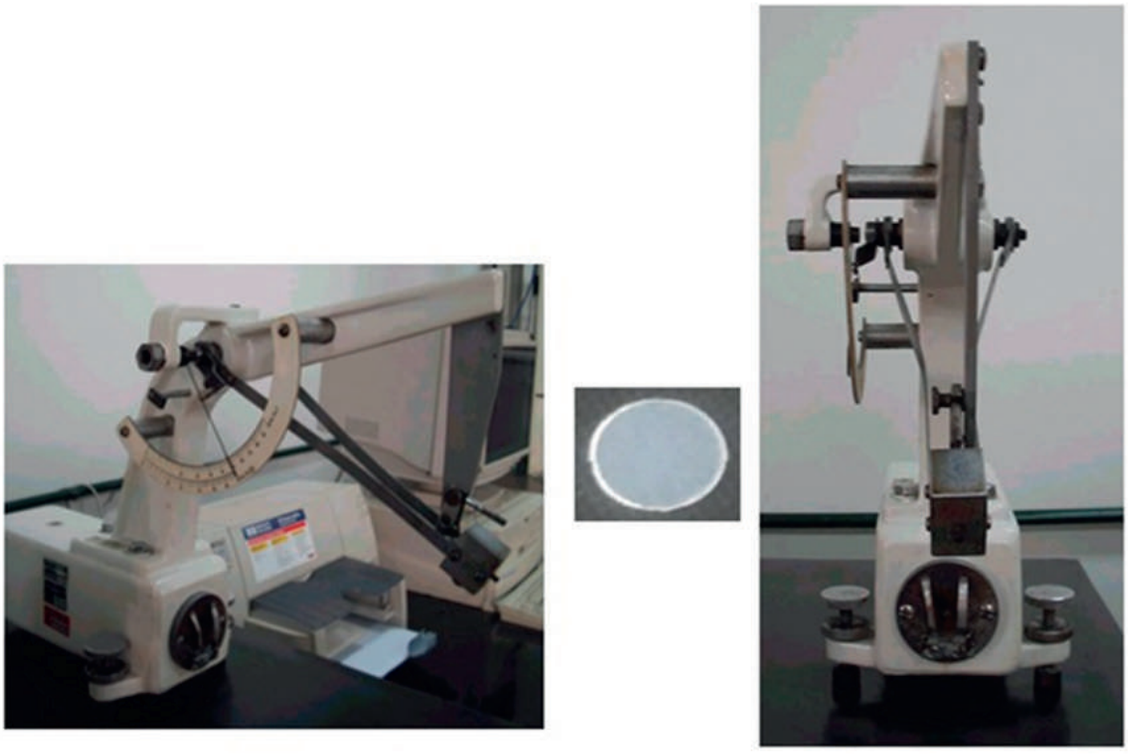

Figure 3. Compression test of the EVA specimens—ABNT NBR 8690—with Schob Pendulum.

In **Figure 3**, the Schob pendulum was used to measure the resilience of the EVA. Six experiments were performed, three used to calibrate the system and three to measure the property. The EVA was observed to have a great damping potential, since it absorbed 50% of the applied energy.

Experimental compression tests were performed to the mechanical characterization of the EVA.

Figure 4 shows the Instron® machine and the recording of the compression tests, performed by a Photron Ultima APX-RS high-speed camera (3000 frames per second). The record helped the study of the nonlinear material behavior of the EVA.

Particularly, **Figure 5** shows that EVA undergoes considerable plastic deformation before failure.

3.1. Mechanical study of the operation of a mouth guard

To reproduce conditions as close as possible to a real situation, models in epoxy resin were manufactured from a patient model (**Figure 6**).

As illustrated in **Figure 7**, the models of the upper and lower arches were fixed in a compression device that allows the lower arch to move while maintaining the upper arch fixed. The compression device was coupled to a Universal Kratos Test Machine, data acquisition system, 20 kN load cell. The aperture, initially in occlusion, was controlled by the extensometer, with a maximum opening of 18 mm. Compression tests were performed, at a velocity of 42.86 mm/min.

http://dx.doi.org/10.5772/intechopen.69969

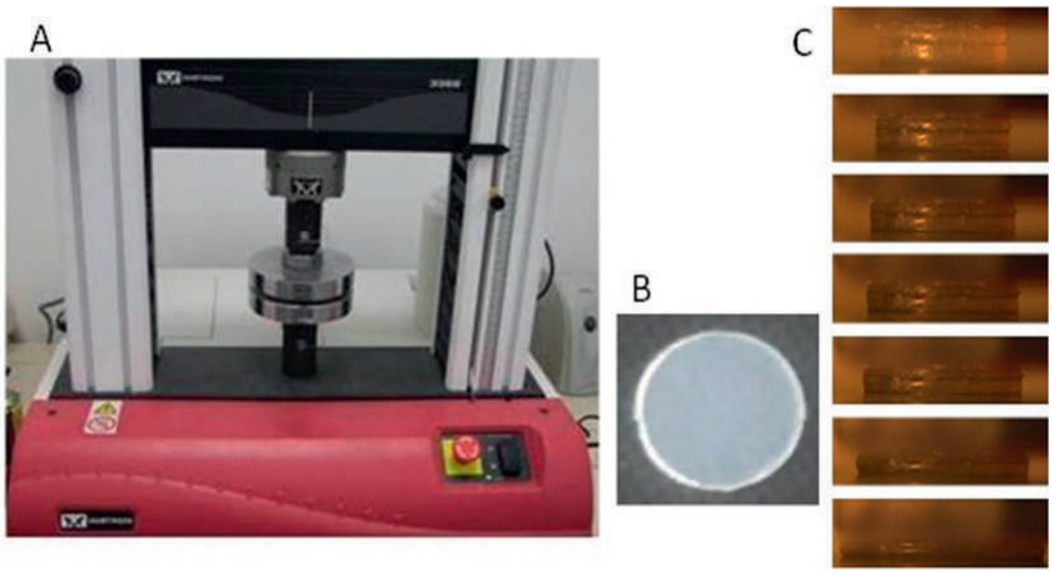

Figure 4. (A) EVA compression test in an Instron machine. (B) Detail of the geometry of the specimen: flat discs with 30 mm in diameter. (C) Compression test recording.

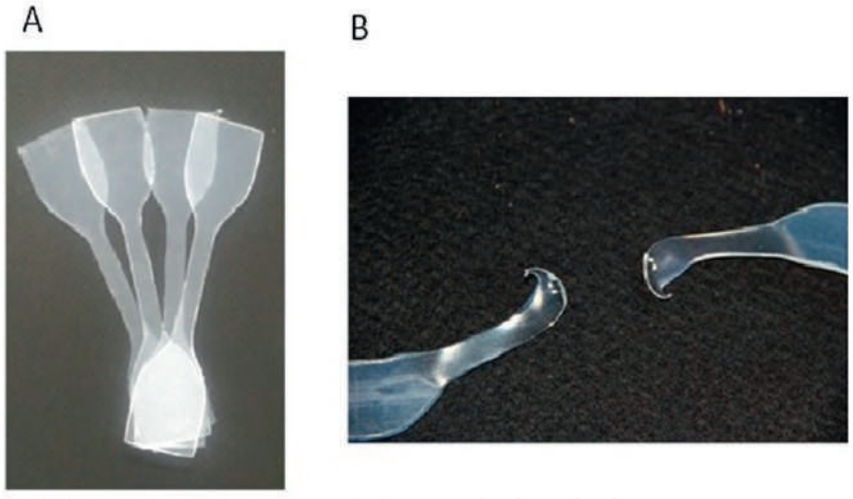

Figure 5. (A) EVA specimens for tensile test. (B) Detail of the specimen after failure.

The test was controlled by optical pyrometer, maintaining the temperature around 37–39°C, close to the mouth temperature (**Figure 8**).

Five EVA mouth guards of each thickness (3 and 4 mm) were made for each test group, using models of a superior dental arch in stone gypsum and metalvander® vacuum-form machine. The geometry respected the recommendation of American Academy for Sports Dentistry [13], that is, 2 mm below the bottom of the vestibular groove, 10 mm beyond the palatine gingival and extension up to the second upper molars.

The heating time for both thicknesses was 4 min, approximately; aspiration time was 45 s (**Figure 9**). All the protectors were immersed in cold water for 10 min.

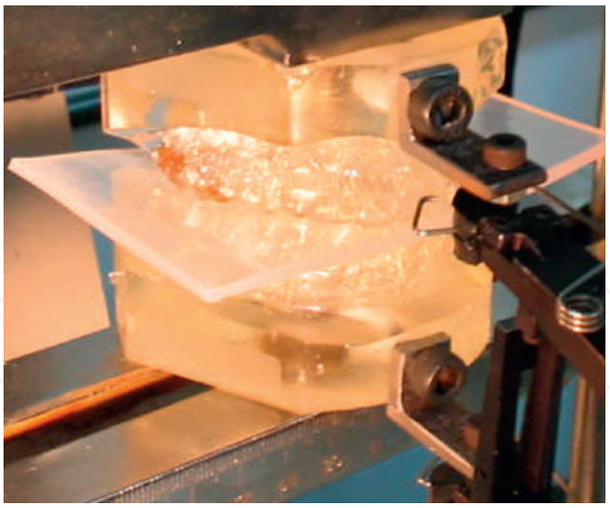

Figure 6. Model of dental arches made of epoxy resin.

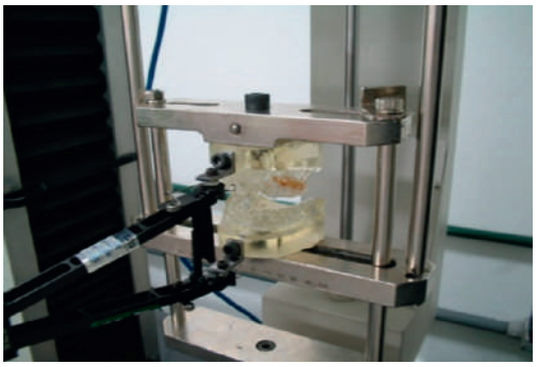

Figure 7. Test set: the Kratos® Universal Testing Machine, dental arch models and extensometer.

Figure 8. Maintenance of the system temperature with an optical pyrometer.

http://dx.doi.org/10.5772/intechopen.69969

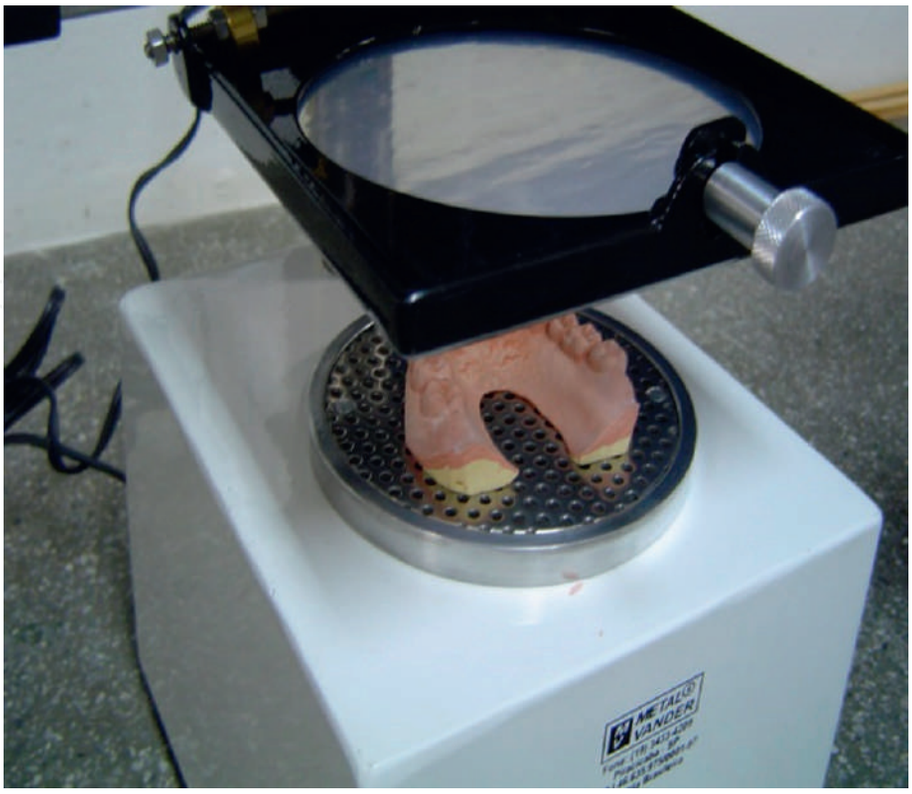

Figure 9. Manufacture of mouth guards in vacuum form Metalvander® machine.

The groups are divided as follows:

A. Mouth guard—3-mm-thick blade

- Room temperature/without saliva
- Room temperature/saturated in saliva
- Oral temperature/without saliva
- Oral temperature/saturated in saliva

B. Mouth guard—4-mm-thick blade

- Room temperature/without saliva
- Room temperature/saturated in saliva
- Oral temperature/without saliva
- Oral temperature/saturated in saliva

Table 1 shows a variation in the compression maximum load in Newtons (N) when evaluating the 3-mm-thick mouth guard (here named $\mathbf{prot}_{\mathbf{A}}$) and the 4-mm-thick mouth guard (here named $\mathbf{prot}_{\mathbf{B}}$).

Coefficient	Max. load (N)	Standard deviation	Significance p
$\mathbf{prot}_A$	2046	20	0.00
$\mathbf{prot}_B$	2219	20	0.00

Table 1. Maximum load variation (N) as a function of the thickness variable, with their respective standard deviations (SD) and significance levels ($p \leq 0.05$), for protectors A and B.

When comparing $\mathbf{prot}_A$ and $\mathbf{prot}_B$ protectors in **Table 1**, $\mathbf{prot}_B$ was observed to require an additional force of 173 N. It agrees with Craig and Godwin [14]: "The energy absorbed in the cyclic moment of compressive deformation should reduce the locally transmitted energy" and thus avoid the rupture of the polymer layer between the teeth. The EVA material acts as a shock absorber, guaranteeing a low energy transmission to the teeth of the dental arch [15].

These data become more relevant when the final measurements of the guard thicknesses are observed. At the end, they presented mean differences in thickness of approximately 0.55 mm, instead of the nominal 1 mm difference. This is already expected, since during the manufacture of the individualized buccal protector there is a loss of thickness between 25 and 50%, also observed in the literature [14, 16]. Analyzing **Table 1** again, one can conclude that a small difference, 0.55 mm, increased the force around 173 N.

4. Numerical analysis of EVA applied to facial protection

Studies in the biological area involving impact have become impossible to perform *in vivo* due to ethical awareness. On the other hand, engineering presented rapid technological development of tools that allow for more detailed analyses, using complex geometries and offering refined results of behavior of virtually modeled bodies [17]. Particularly, the finite element method (FEM) is a powerful tool, able to virtually mimic different complex phenomena, including the impact of an object on a human face.

However, to analyze the performance of different EVA geometries and properties (flexible and rigid forms) via FEM, it is necessary to determine the parameters and constitutive laws for the materials (tissue, bone, EVA), geometry of the studied problem (face and projectile) and boundary conditions (initial velocity of the projectile, displacement restrictions in the system).

4.1. Material parameters and constitutive laws

4.1.1. Face bones

Most of the bony framework of the face has high-level resistance, since it protects vital elements, such as the brain, the eyes and the neuromuscular structures. Yet, it is also composed of very fragile bones, such as the maxilla, nasal bones and the malar portion of the zygomatic bone [18–22].

http://dx.doi.org/10.5772/intechopen.69969

When a facial bone is fractured, undergoing or not surgery reduction, it should not be exposed to any trauma during the bone healing process, which lasts about 30 days [23–27]. If surgical reduction is required, it should occur within the first 2–3 h after the injury occurs [28, 29].

Cases of surgical reduction may disrupt the performance of athletes. In these cases, the use of the facial protector can allow an early and safe return of the athlete to training and competitions [22, 27, 28, 30]. In general, 4–7 days are required for the face molding and for manufacturing/producing the protector.

For the present FEM analysis, the cortical bone is represented as a linear elastic, homogeneous and isotropic material. The mechanical properties—density, Young's modulus, Poisson coefficient and maximum strength—of each bone depend on its composition, as reported by Lotti et al., Handbook in 2006 [31].

Table 2 presents the maximum compressive load of each bone portion of interest for dentistry. Particularly for the cortical bone, the elastic material parameters are listed in **Table 3**.

4.1.2. Human soft tissue

The soft tissue named here is composed of the skin and the muscular portion of the studied region.

The soft tissue is a hyperelastic nonlinear material [33–37] here represented by the well-known Ogden model [35, 37].

Table 4 lists the parameters used for soft tissue in the FEA. The elastic parameters are the same as those adopted by several car manufacturers to simulate pedestrian—car impact—and Ogden parameters were obtained by Coto et al. [6], according to the definition in the finite-element software LS-Dyna.

Bone	Max. load (N)	Max compressive stress (N/mm^2)
Frontal	1000–6494	≥7.58
Zygomatic	489–2401	1.38–4.17
Mandible	668–1801	1.03–2.07
Nasal	342–450	0.13–0.34

Table 2. Face bone resistance [32].

Structure	Young Modulus (MPa)	Poisson coefficient	Density (t/mm^3)
Cortical bone	13,700	0.32	2.28

Table 3. Elastic parameters for the cortical bone.

	Elastic parameters			Ogden parameters	
	Shear Modulus (MPa)	**Poisson coefficient**	**Density (t/mm³)**	μ_1/α_1	μ_2/α_2
Tissue	0.69	0.495	1.438 E – 9	7.0/0.8	2.6/2.6

Table 4. Material model for human tissue.

4.1.3. Flexible EVA

Flexible EVA has high elasticity and low mechanical resistance. A reverse analysis method was adopted to extract the material properties from the experimental tests described. In the reverse method, material parameters are tuned such that numerical predictions match the experimental curves (**Figure 10**).

Table 5 summarizes the material parameters, used to characterize flexible EVA, according to the Ogden hyperelastic model, available in the commercial software LS-Dyna® and adopted in this study.

4.1.4. Rigid EVA

The inverse methodology was again adopted here, to characterize rigid EVA. **Figure 11** shows the similarity between the experimental and the numerical compression tests.

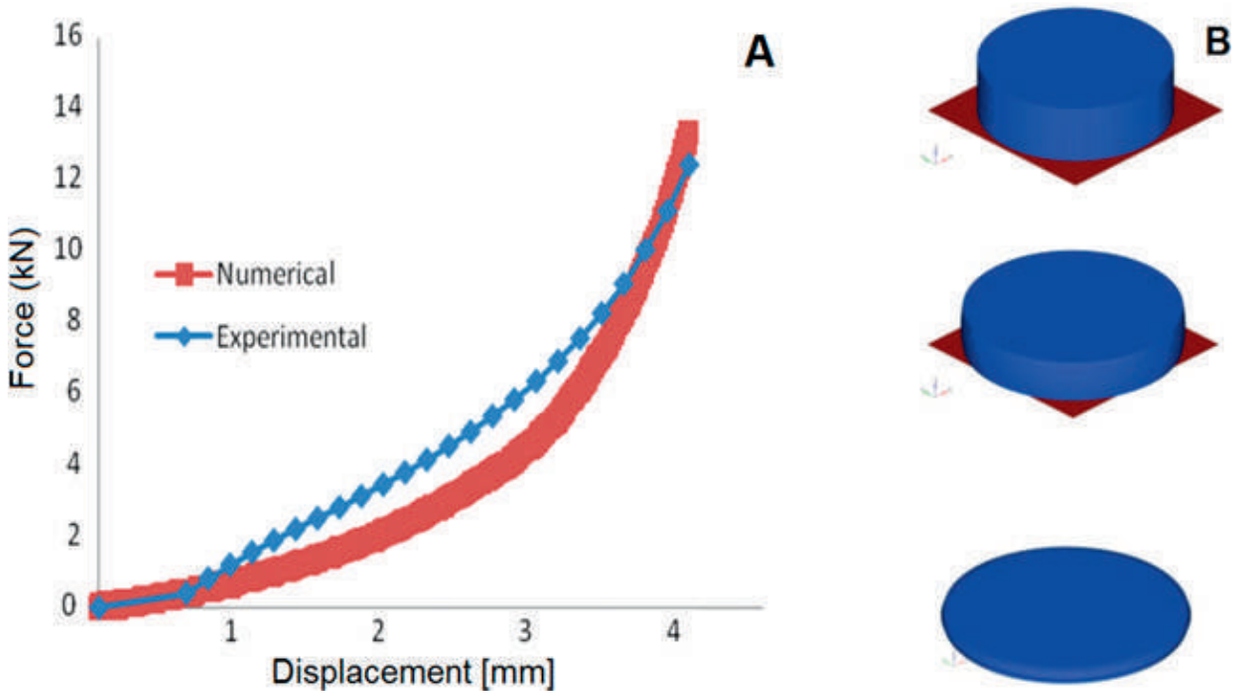

Figure 10. (A) Experimental and numerical curve for compression test. (B) Specimen configuration at different instants of the numerical analysis [6].

	μ_1/α_1	μ_2/α_2	Poisson coefficient	Shear Modulus (MPa)	Density (t/mm³)
Flexible EVA	7.0/0.8	2.6/2.6	0.48	10.0	2.0 E − 9

Table 5. The material model for flexible EVA.

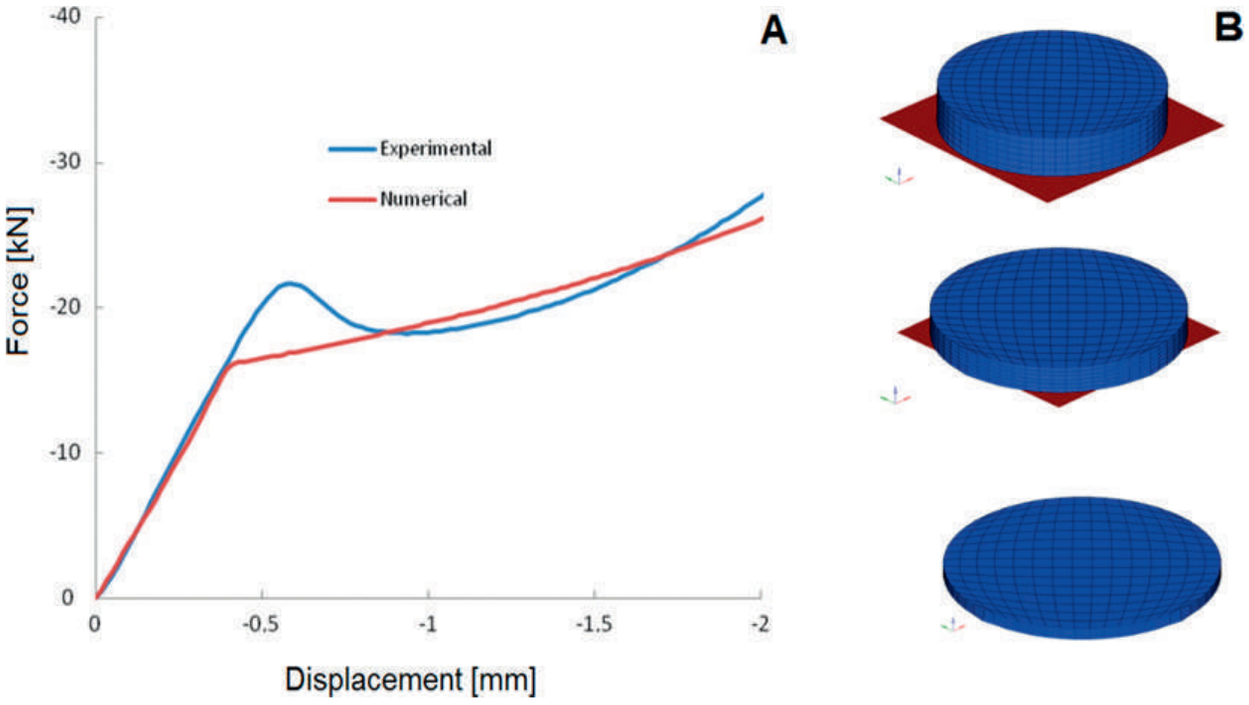

Figure 11. (A) Experimental and numerical curve for compression tests of rigid EVA. (B) Specimen configuration at different instants of the numerical analysis [37].

Table 6 shows the material parameters used for the rigid EVA, according to the Ogden model available in the software LS-Dyna®.

4.1.5. Geometry

As for numerical simulations of the human face, the geometry is a challenge, due to the great number of particularities.

To overcome this problem, a scientific partnership was established with the Renato Archer Information Technology Center (CTI Renato Archer). They provided the face images (**Figure 12**), obtained by computerized tomography (CT) and using in-house software.

	μ_1/α_1	μ_2/α_2	Poisson coefficient	Shear Modulus (MPa)	Density (t/mm³)
Rigid EVA	1.0/0.05	10.0/−4.0	0.49	175	1.2 E − 9

Table 6. Material model for rigid EVA.

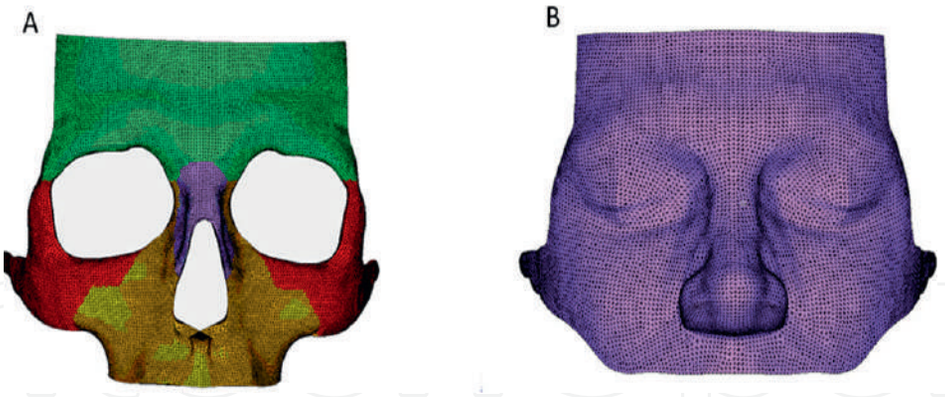

Figure 12. (A) The bone and (B) soft tissue configuration of the face, obtained from CT [37].

4.2. Numerical analyses

Using the material and geometrical parameters defined so far, it is possible to perform complex numerical analyses of the face, with different load conditions. Here, software LS-Dyna was used. The mesh generation and data analyses were performed with the pre- and post-processors HyperMesh and HyperView, respectively [38, 39].

4.2.1. EVA as nasal protector for sport

Coto et al. [6] studied the performance of EVA nasal protectors undergoing the impact of a rigid ball in the face with a 3D FE model (**Figure 13**). The material used was a combination of 1 mm of rigid EVA with 2 mm of flexible EVA. The author concluded that the proposed protector could absorb and dissipate the energy from the impact of a ball with mass of 0.025 kg at initial velocity of 20 m/s. The energy is high enough to fracture the nasal bone if there is no protector (**Figure 14**).

According to Coto et al. [37], rigid EVA reduced the velocity of impact and the flexible EVA increased the time interval of the impulse, thus decreasing the peak load transmitted to the bone.

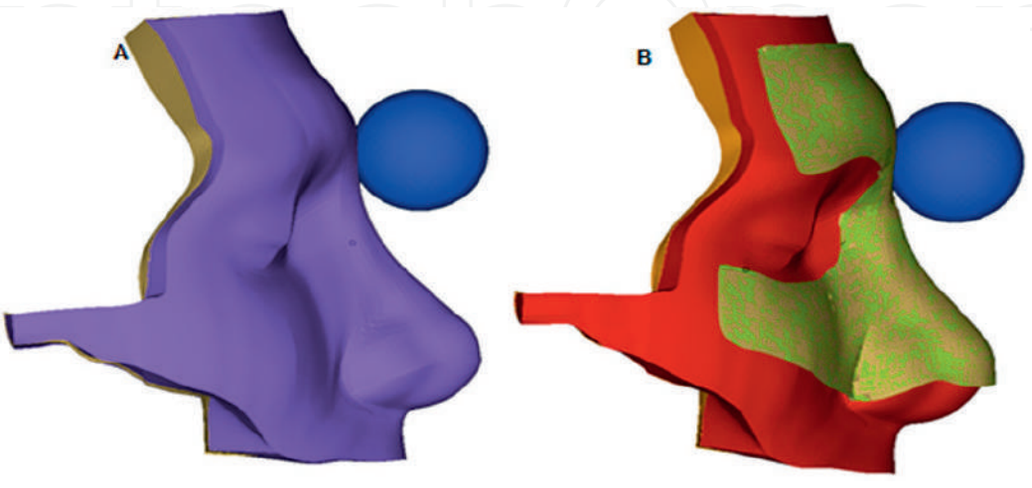

Figure 13. FE model. (A) Without the protector. (B) With the protector. Figure is extracted from Coto et al. [37].

http://dx.doi.org/10.5772/intechopen.69969

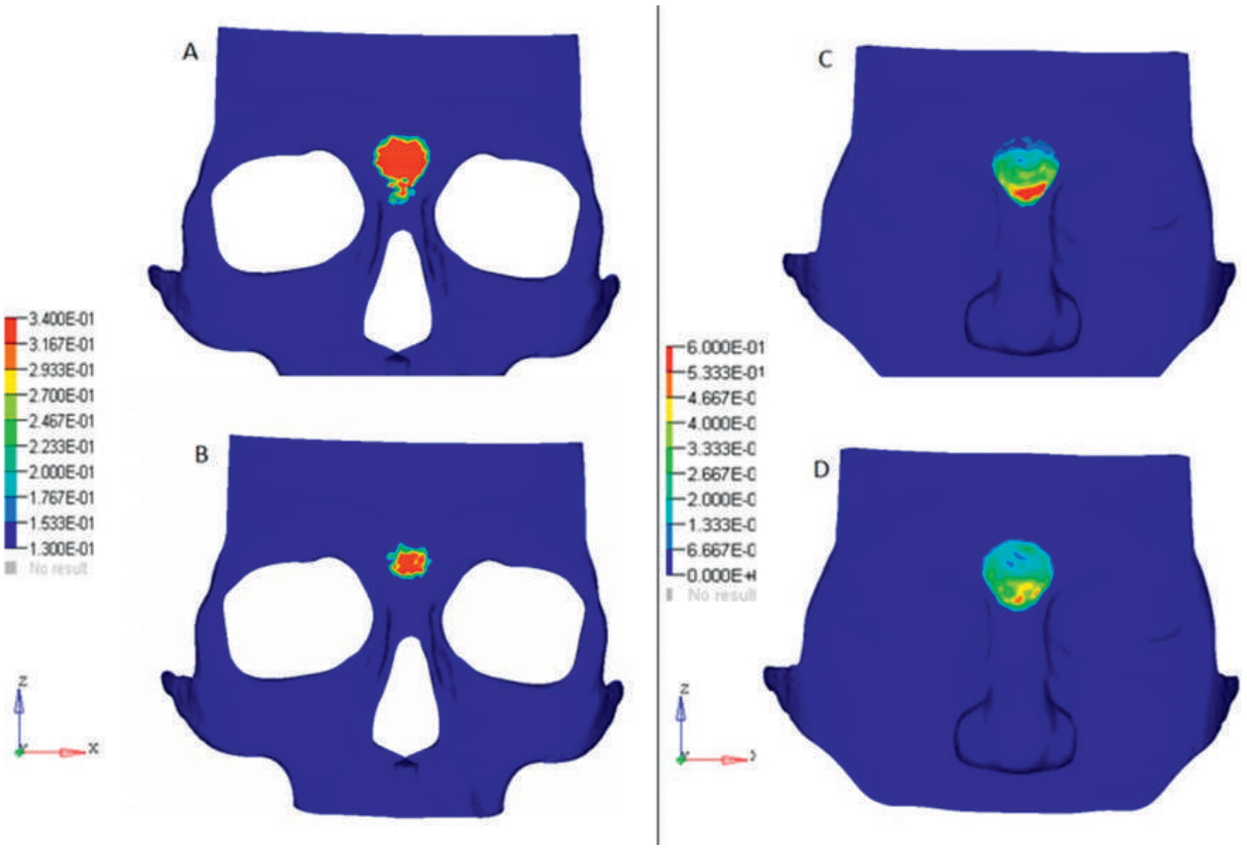

Figure 14. (A, B) Normal compressive stress in the bones of the frontal region, after impact, (A) without and (B) with nasal protector. (C, D) Normal compressive stress in the soft tissue of the frontal region, after the impact, (C) without protector and (D) with protector. Figure is extracted from Coto et al. [37].

4.3. Study of EVA to protect the zygomatic bone

The zygomatic bone forms the prominence of the cheek, part of the lateral wall and floor of the orbit. Due to its location and prominence, it presents a high risk of fracture [39–41]. The thickness is not constant in its extension. The zygomatic bone is composed of cortical and spongy bone in the thicker portion, and in the region near the frontonasal suture, it is almost exclusively formed by the cortical bone [41].

A simplified geometry of overlapping discs with a 100-mm radius was considered. The layers were composed of bone tissue (zygomatic bone portion, lower malar portion, near the nasal front suture), soft tissue and three proposed rigid and flexible EVA combinations, according to **Table 7**.

	Flexible EVA (thickness, mm)	Rigid EVA (thickness, mm)	Flexible EVA (thickness, mm)
G1	2	1	1
G2	3	1	–
G3	2	1	–

Table 7. Configurations analyzed for rigid and flexible EVA.

Figure 15 shows the geometry for G1. An extra configuration formed only by the cortical bone and soft tissue was also included in the analyses as a control group (CG) as shown in **Figure 16**.

Figure 16 also shows the projectile, here represented by a golf ball, with parameters obtained in Bartlett et al. [43] (**Table 8**). The ball had a velocity of 10 m/s at the instant of impact.

The parameters used for the cortical bone, soft tissue, flexible and rigid EVA are in **Tables 3–6**, respectively. The thicknesses of bone and soft tissue were 10.3 mm [42] and 12.3 mm [43], respectively.

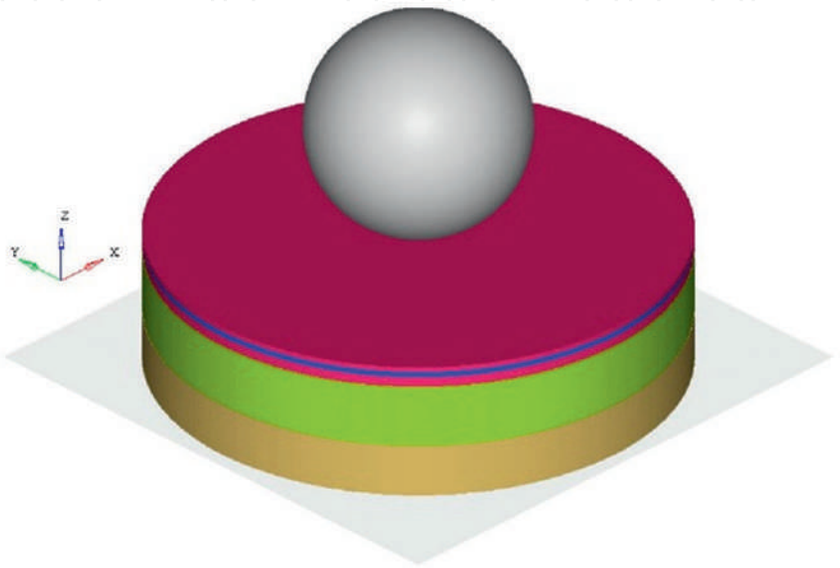

Figure 15. Simplified geometry (Group G1), soft EVA, rigid EVA, soft tissue amd bone.

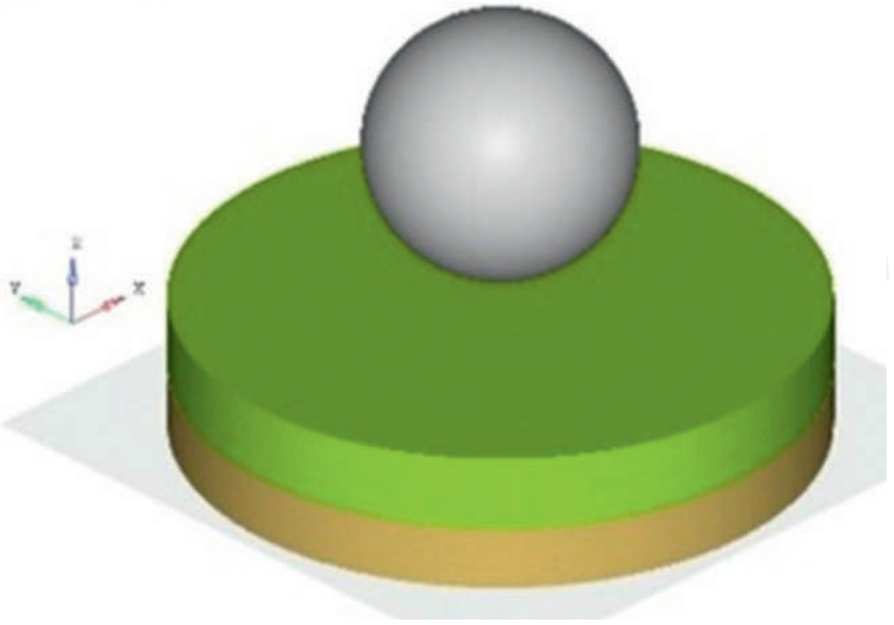

Figure 16. Control Group (CG), soft tissue and zigomatic bone.

http://dx.doi.org/10.5772/intechopen.69969

	Young Modulus (MPa)	Poisson coefficient	Density (t/mm^3)	Radius (mm)	Velocity (m/s)
Golf ball	392	0.45	1.15 E − 9	21	10

Table 8. Geometric and material characteristics of the projectile.

The analyses were performed by the LS-Dyna software. The minimum compression stress was controlled. The maximum pressure allowed for the bone and the EVA (rigid or flexible) was of 2.7 MPa and 5.0 MPa, respectively. The friction value considered was 0.5 between ball and soft tissue.

5. FEA results

Figure 17 shows the pressure for the CG. The figure shows the high level of pressure at the zygomatic bone, exceeding the failure limit of 2.7 MPa.

According to the analyses, the results showed that in the three models proposed, there was the maximum performance of EVA, but the best protection to the studied bone is given by the G2 model. **Figure 18** shows the pressure profile in the EVA for G1 and G3.

Figure 19 shows the energy conversion during impact in G2.

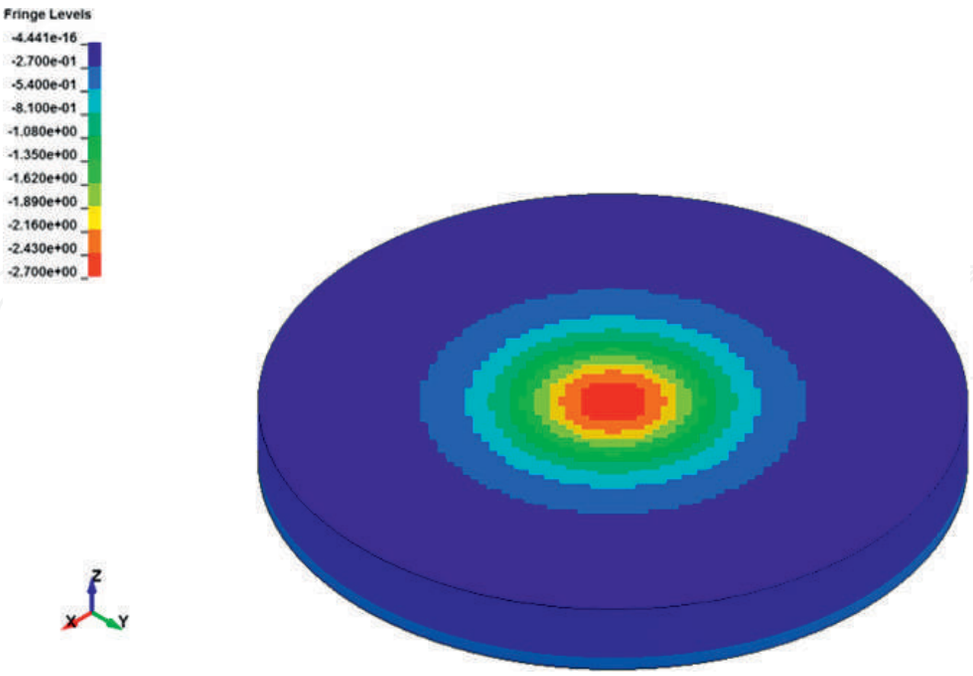

Figure 17. Pressure for the CG.

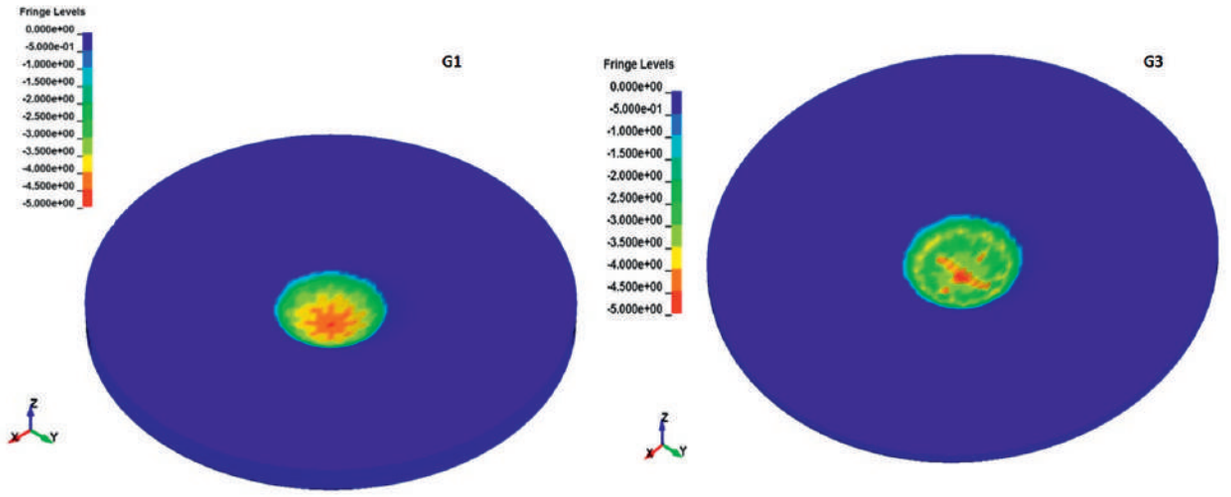

Figure 18. Results of pressure profile in the protector for G1 and G3, respectively.

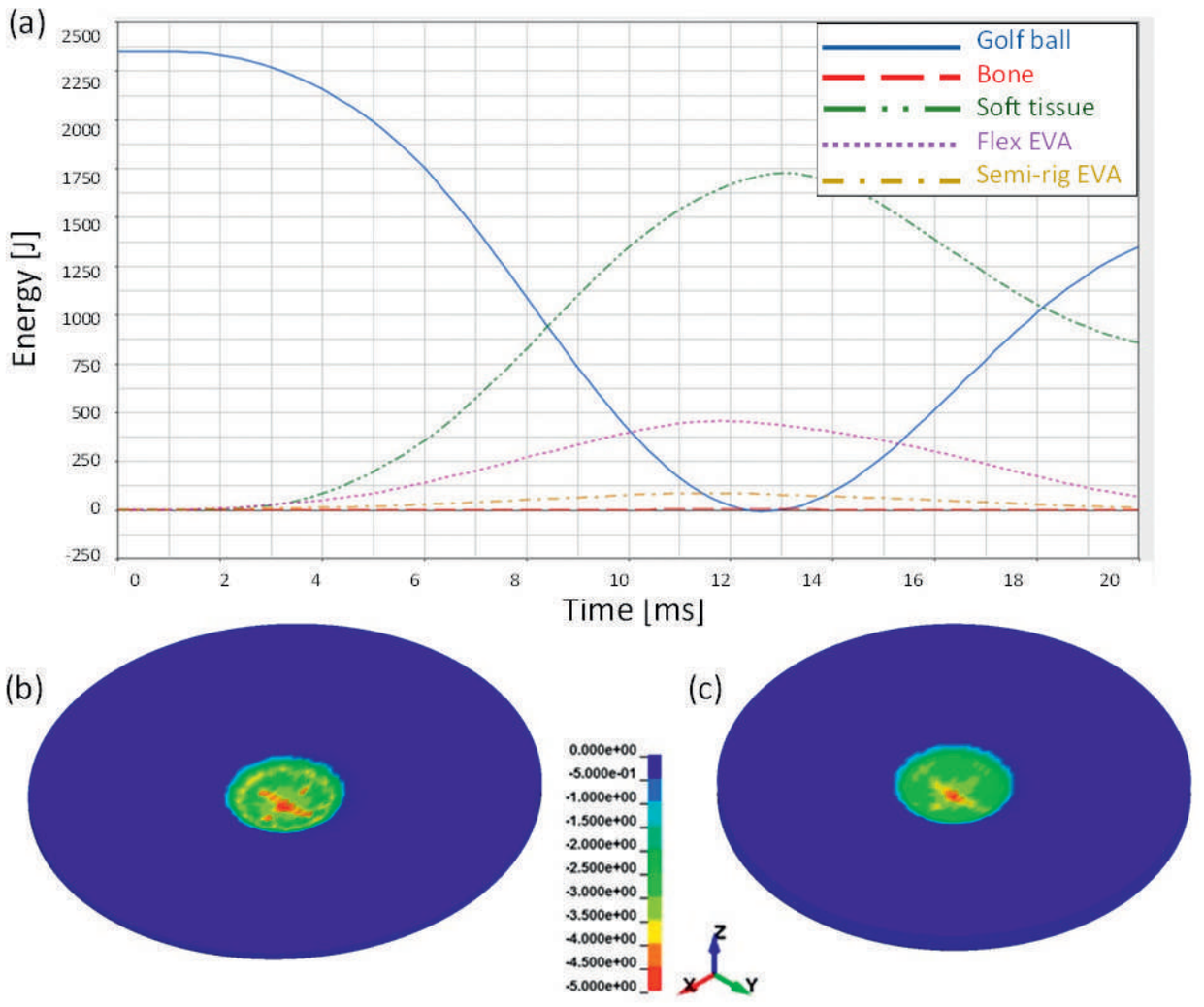

Figure 19. (a) Energy conversion during impact for G2; pressure in the (b) semirigid and (c) flexible EVA.

6. Conclusions

In human health science research, the study of materials that may replace organs is in constant evolution. Particularly in dentistry, the material should be easy to manipulate, esthetically acceptable, stable to use in the oral environment, in the presence of saliva and chewing conditions and low cost. Moreover, mechanical, physical, chemical and biological properties of any material used in the area must be known.

EVA was the object of this study. It is a thermoplastic copolymer derived from petroleum.

Initially, the material was studied in the mouth environment, and it was mechanically and chemically characterized. Finally, the material is molded and applied to facial protection.

The application is numerical, since studies in the biological area involving impact have become impossible to perform *in vivo*. FEM is a powerful tool, able to virtually mimic different complex phenomena. The quality of the results strongly depends on the correct material characterization, precise geometry of the analyzed structure and real boundary conditions (initial velocity of the projectile, displacement restrictions in the system).

The facial protector was tested during the impact of a golf ball in the nasal bone and, through a simplified model, in the zygomatic bone. The proposed protector is able to amortize the impact, and its configuration does not compromise peripheral view and does not cause discomfort to the athlete.

Author details

Reinaldo Brito e Dias[1], Neide Pena Coto[1]*, Gilmar Ferreira Batalha[2] and Larissa Driemeier[2]

*Address all correspondence to: neidecoto@gmail.com

1 School of Dentistry, University of São Paulo, Sao Paulo, Brazil

2 School of Engineering, University of São Paulo, Sao Paulo, Brazil

References

[1] WHO. Available from: http://www.direitoshumanos.usp.br/index.php/OMS-Organização-Mundial-da-Saúde/constituicao-da-organizacao-mundial-da-saude-omswho.html. 2014. [Accessed: June 10, 2014]

[2] Anusavice KJ, Shen C, Rawls R. Phillips materiais dentários. [Roberto Braga, et al. (translator)]. 12th ed. Rio de Janeiro: Elsevier; 2013

[3] Wong EW, White RC. Development of a shock absorbing biomedical elastomer for a new total elbow replacement design. Biomaterials, Medical Devices, and Artificial Organs. 1979;**7**(2):283-290

[4] Coto NP, Dias RB, Costa RA, Antoniazzi TF, de Carvalho EP. Mechanical behavior of ethylene vinyl acetate copolymer (EVA) used for fabrication of mouthguards and inter-occlusal splints. Brazilian Dental Journal. 2007;**18**(4):324-328

[5] Rawls RH. Polimeros odontológicos. In: Nausavice KJ, editor. Phillips materiais dentários. 11th ed. Rio de Janeiro: Elsevier; 2005. pp. 135-157

[6] Coto NP, Meira JBC, Dias RB, Driemeier L, Roveri GO, Noritomi PY. Assessment of nose protector for sport activities: Finite element analysis. Dental Traumatology. 2012 Apr;**28**(2):108-113

[7] Bugada DC, Rudin A. Molecular structure and melting behaviour of ethylene-vinyl acetate copolymers. European Polymer Journal. 1992;**28**(3):219-227

[8] Bhowmick AK, Stephens HL. Handbook of Elastomers—News Developments and Technology. New York: Marcel Dekker; 1988

[9] Zhang X, Zhou Q, Liu H, Liu H. UV light induced plasticization and light activated shape memory of spiropyran doped ethylene-vinyl acetate copolymers. Soft Matter. 2014 Jun 7;**10**(21):3748-3754

[10] Bishop BM, Davies EH, Von Fraunhofer JA. Materials for mouth protector. Journal of Prosthetic Dentistry. 1985;**53**(13):256-261

[11] Chen CP, Lakes RS. Design of viscoelastic impact absorbers: Optimal material property. International Journal of Solids and Structures. 1990;**26**(12):1313-1328

[12] Hoffman J, Alfter G, Rudolph NH, Göz G. Experimental comparative study of various mouth guards. Endodontics & Dental Traumatology. 1999;**15**:157-163

[13] Sports Dentistry Academy [online]. Types of Athletic Mouthguards. 2005. Available from: http.sportsdentistry.com [Accessed: June 4, 2005]

[14] Craig RG, Godwin WC. Physical properties of material for custom made mouth protectors. Journal of the Michigan State Dental Association. 1967;**47**:34-40

[15] Hans GE. An Introduction to Plastics. Weinheim, New York: VHC; 1993

[16] Park MS, Levy ML. Biomechanical aspects of sports-related head injuries. Neurologic Clinics. 2008 Feb;**26**(1):33-43

[17] Matsumoto AT, Driemeier L, Alves M. Performance of polymer reinforcements in vehicle structures submitted to frontal impact. International Journal of Crashworthiness. 2012;**17**:479-496

[18] Le Fort R. Êtude experimentale sur les fractures de la machoire superieure. Revue Chir de Paris. 1901;**23**:208-306

[19] Stanley RB Jr, Nowak GM. Midfacial fractures: Importance of angle of impact to horizontal craniofacial buttresses. Otolaryngology—Head and Neck Surgery. 1985 Apr; **93**(2):186-192

[20] Delilbasi C, Yamazawa M, Nomura K, Lida S, Kogo M. Maxillofacial fractures sustained during sports played with a ball. Oral Surgery, Oral Medicine, Oral Pathology, Oral Radiology, and Endodontology. 2004 Jan;**97**(1):23-27

[21] Higuera S, Lee EI, Cole P, Hollier LH Jr, Stal S. Nasal trauma and the deviated nose. Plastic and Reconstructive Surgery. 2007 Dec;**120**(7 Suppl 2):64S-75S

[22] Chao MT, Paletta C, Garza JR. Facial trauma, sports-related injuries. Medscape Journal of Medicine. 2008;**1**:1-14

[23] Ellis E 3rd, Kittidumkerng W. Analysis of treatment for isolated zygomatic maxillary complex fractures. Journal of Oral and Maxillofacial Surgery. 1996 Apr;**54**(4):386-400

[24] Garza JR, Baratta RV, Odinet K, Metzinger S, Bailey D, Best R, et al. Impact tolerances of the rigidly fixated maxillofacial skeleton. Annals of Plastic Surgery. 1993 Mar;**30**(3):212-216

[25] Levin L, Friedlander LD, Geiger SB. Dental and oral trauma and mouthguard use during sport activities in Israel. Dental Traumatology. 2003 Oct;**19**(5):237-242

[26] Ranalli DN, Demas PN. Orofacial injuries from sport: Preventive measures for sports medicine. Sports Medicine. 2002;**32**(7):409-418

[27] Cascone P, Petrucci B, Ramieri V, Marianetti TM. Security hi-tech individual extra-light device mask: A new protection for [soccer] players. Journal of Craniofacial Surgery. 2008 May;**19**(3):772-776

[28] Dingman RO, Natvig P. Cirurgia das fraturas faciais. São Paulo: Editora Santos; 2001

[29] Crow RW. Diagnosis and management of sports-related injuries to the face. Dental Clinics of North America. 1991 Oct;**35**(4):719-732

[30] Morita R, Shimada K, Kawakami S. Facial protection masks after fracture treatment of the nasal bone to prevent re-injury in contact sports. Journal of Craniofacial Surgery. 2007 Jan;**18**(1):143-145

[31] Handbook ES. Coefficients of Friction—Many Material Compared. 2006;**18**:942

[32] Hodgson VR. Tolerance of the facial bones to impact. American Journal of Anatomy. 1967;**120**:113-122

[33] Miller K, Chinzei K. Constitutive modelling of brain tissue: Experiment and theory. Journal of Biomechanics. 1997 Nov–Dec;**30**(11-12):1115-1121

[34] Verdejo R, Mills NJ. Heel-shoe interactions and the durability of EVA foam running-shoe midsoles. Journal of Biomechanics. 2004 Sep;**37**(9):1379-1386

[35] Gerard JM, Ohayon J, Luboz V, Perrier P, Payan Y. Non-linear elastic properties of the lingual and facial tissues assessed by indentation technique. Application to the biomechanics of speech production. Medical Engineering & Physics. 2005 Dec;**27**(10):884-892

[36] Zahouani H, Pailler-Mattei C, Sohm B, Vargiolu R, Cenizo V, Debret R. Characterization of the mechanical properties of a dermal equivalent compared with human skin in

vivo by indentation and static friction tests. Skin Research and Technology. 2009 Feb; **15**(1):68-76

[37] Coto NP, Driemeier L, Roveri GO, Meira JBC, Dias RB, Noritomi PY. Numerical study of the face bone behaviour when impacted by rigid ball. Journal of Biomechanics. 2012 Jul;**45**:1121

[38] Withnall C, Shewchenko N, Gittens R, Dvorak J. Biomechanical investigation of head impacts in football. British Journal of Sports Medicine. 2005 Aug;**39**(Suppl 1):i49-i57

[39] Verschueren P, Delye H, Depreitere B, Van Lierde C, Haex B, Berckmans D. A new test set-up for skull fracture characterisation. Journal of Biomechanics. 2007;**40**(15):3389-3396

[40] Gialain IO, Dias RB, Coto NP. Mouthguard: A new technique for the partially edentulous patient. Dental Traumatology. 2014 Oct;**30**(5):411-414

[41] Del Neri NB, Araujo-Pires AC, Andreo JC, Rubira-Bullen IR, Ferreira Júnior O. Zygomaticofacial foramen location accuracy and reliability in cone-beam computed tomography. Acta Odontologica Scandinavica. 2014 Feb;**72**(2):157-160

[42] de Almeida NH, Michel-Crosato E, de Paiva LA, Biazevic MG. Facial soft tissue thickness in the Brazilian population: New reference data and anatomical landmarks. Forensic Science International. 2013 Sep 10;**231**(1-3):404

[43] Bartlett R, Gratton C, Rolf CG, editors. Encyclopedia of International Sports Studies. Abington: Routledge; 1987

Chapter 15

Tailoring Bioengineered Scaffolds for Regenerative Medicine

Sandra Amado, Pedro Morouço,
Paula Pascoal-Faria and Nuno Alves

Additional information is available at the end of the chapter

http://dx.doi.org/10.5772/intechopen.69857

Abstract

The vision to unravel and develop biological healing mechanisms based on evolving molecular and cellular technologies has led to a worldwide scientific endeavor to establish regenerative medicine. This is a multidisciplinary field that involves basic and preclinical research and development on the repair, replacement, and regrowth or regeneration of cells, tissues, or organs in both diseases (congenital or acquired) and traumas. A total of over 63,000 patients were officially placed on organs' waiting lists on 31 December 2013 in the European Union (European Commission, 2014). Tissue engineering and regenerative medicine have emerged as promising fields to achieve proper solutions for these concerns. However, we are far from having patient-specific tissue engineering scaffolds that mimic the native tissue regarding both structure and function. The proposed chapter is a qualitative review over the biomaterials, processes, and scaffold designs for tailored bioprinting. Relevant literature on bioengineered scaffolds for regenerative medicine will be updated. It is well known that mechanical properties play significant effects on biologic behavior which highlight the importance of an extensively discussion on tailoring biomechanical properties for bioengineered scaffolds. The following topics will be discussed: scaffold design, biomaterials and scaffolds bioactivity, biofabrication processes, scaffolds biodegradability, and cell viability. Moreover, new insights will be pointed out.

Keywords: tailored scaffold, biomaterials, bioprinting, biomechanics, regenerative medicine

1. Introduction

In a society that is in constant development, the discovery of "new" scientific and technological knowledge must (i) progress at an incredibly fast pace, (ii) target a wide audience, and (iii) have a practical impact in the society. The health sciences are naturally a priority area of

research, mostly because of the impact they have on the augment human life expectancy, by developing advanced and patient-specific therapies.

Only the complexity of human tissues could justify that in the 1980s tissue engineering emerged as a scientific field with an enormous potential. Targeting to regenerate the bone, cartilage, skin, or other tissues and organs, bridging the anatomy with its physiology/function is a paramount challenge to be solved. Several efforts have been made, by research groups spread worldwide, to tailor bioengineering scaffolds (sometimes denominated by tissue constructs) that could mimic native tissues. However, the achievement of three-dimensional (3D) complex organ structures is far from being tangible. Due to its nature, tissue engineering gathers scientists, engineers, and physicians in multidisciplinary teams using a variety of methods to construct biological substitutes [1]. Indeed, significant efforts are being developed worldwide in the fields of tissue engineering and regenerative medicine, but full tissue or organ regeneration remains a paramount challenge. Therefore, these multidisciplinary scientific fields apply a wide variety of methodologies, where multidisciplinary research teams can provide suitable inputs for its development [2].

One of the major goals is to produce biological substitutes to restore, maintain, or improve tissue function, using biocompatible and biodegradable support structures, i.e., scaffolds, in conjunction with human cells (**Figure 1**) [3]. Gathering tissue engineering and regenerative medicine, researchers have been interested on developing alternative approaches for restoring functionality. To do so, one of the most promising methodologies involves the use of additive manufacturing (AM) processes. AM technologies allow the production of complex 3D structures concerning mainly a high level of control, predefined geometry, size, and interconnected pores in a reproducible way. This optimized controlled organization enhances the vascularization and, thus, transports oxygen and nutrients throughout the whole structure,

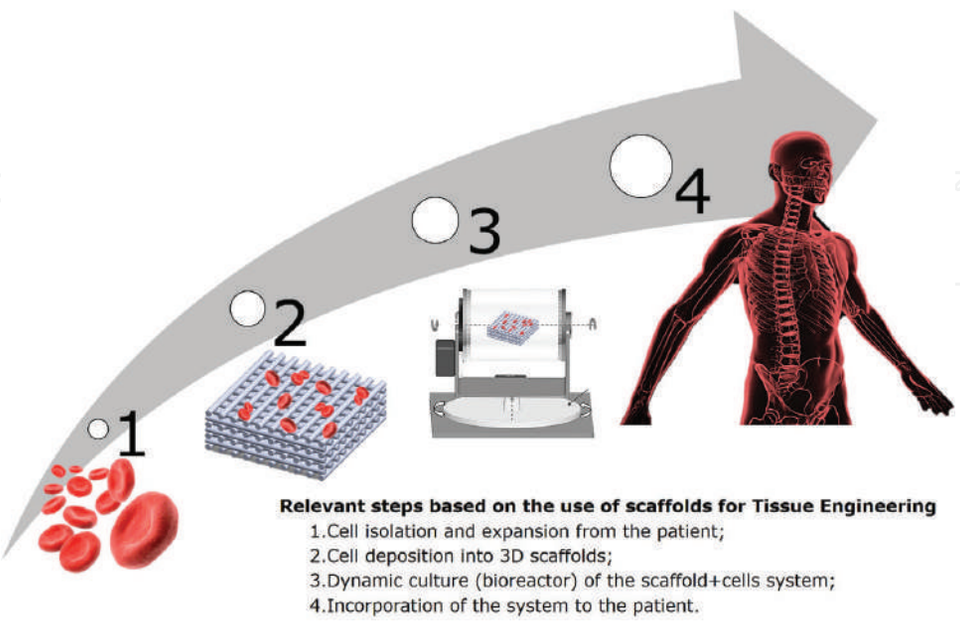

Figure 1. Relevant steps based on the use of scaffolds for tissue engineering.

providing an adequate biomechanical environment for tissue regeneration [4]. However, adapting the adequate technology with enhanced biomaterials, in order to obtain customized implants that mimic the native tissue, is nowadays a challenge with a huge potential.

This chapter intends to provide a synopses in patient-specific engineering scaffolds. A revision of the scaffold design, biomaterials, and advanced manufacturing processes will help to establish new research paradigms on tailoring bioengineered scaffolds for regenerative medicine. Recent advances will be highlighted to stimulate the readers for future insights and possibilities.

2. Scaffold design

Scaffold modeling plays a key role in tissue engineering and regenerative medicine. A well-designed 3D scaffold is a fundamental tool to guide tissue formation both in vitro and in vivo. Properties such as high surface-area-to-volume ratio, porosity, pore size, pore design, pore interconnectivity, permeability, and degradation should be taken into account when designing scaffold for different and tailored applications. These will allow a desirable biological network for cell migration, nutrient transportation, and the mechanical stiffness, and strength can be therefore obtained [5, 6]. Growth factors (GFs) and drug release (DR) should also be considered to achieve an optimized tissue growth as scaffold degraded. Moreover, some authors have shown the benefits for tissue generation of using curvature and concave surfaces compared to convex and planar ones [7].

To address and fulfill aforementioned requirements, two scaffold design approaches can be used according to the flowchart presented in **Figure 2**. The first one is based on the native tissue, whereas the second one is based on the unit digital cell model, both addressing tailored scaffold geometry. The geometry obtained can then be used on computer-aided engineering studies to optimize the performance of the tailored bioengineering scaffold. Finally, a physical optimized scaffold can be produced using 3D printing or AM technology before in vitro and/or in vivo implantation of the scaffold. Accordingly, several research works have been developed concerning tailored scaffold geometry and its fabrication. In these studies, physical scaffolds have been used directly for in vitro and/or in vivo studies. Nevertheless, the link between computer modeling and computer-aided engineering to tailor bioengineering scaffold remains a paramount challenge. When solved, it can significantly reduce animal experimental studies.

In the computer modeling based on native tissue, different noninvasive 3D scanning techniques can be considered to obtain the 3D anatomical geometric model. The most used are computed tomography (CT), μCT (micro-CT), and nCT (nano-CT), which considered different scale levels [8–10], as well as magnetic resonance image (MRI) and 3D optical techniques. All these techniques used different physical principles to obtain a series of two-dimensional (2D) images or a 3D point cloud of the sample of the native tissue studied. CT requires the exposition of the sample of the native tissue to ionizing radiation, whereas MRI uses a magnetic field and pulses of radio wave energy (avoiding radiation) both obtaining a series of 2D images. In

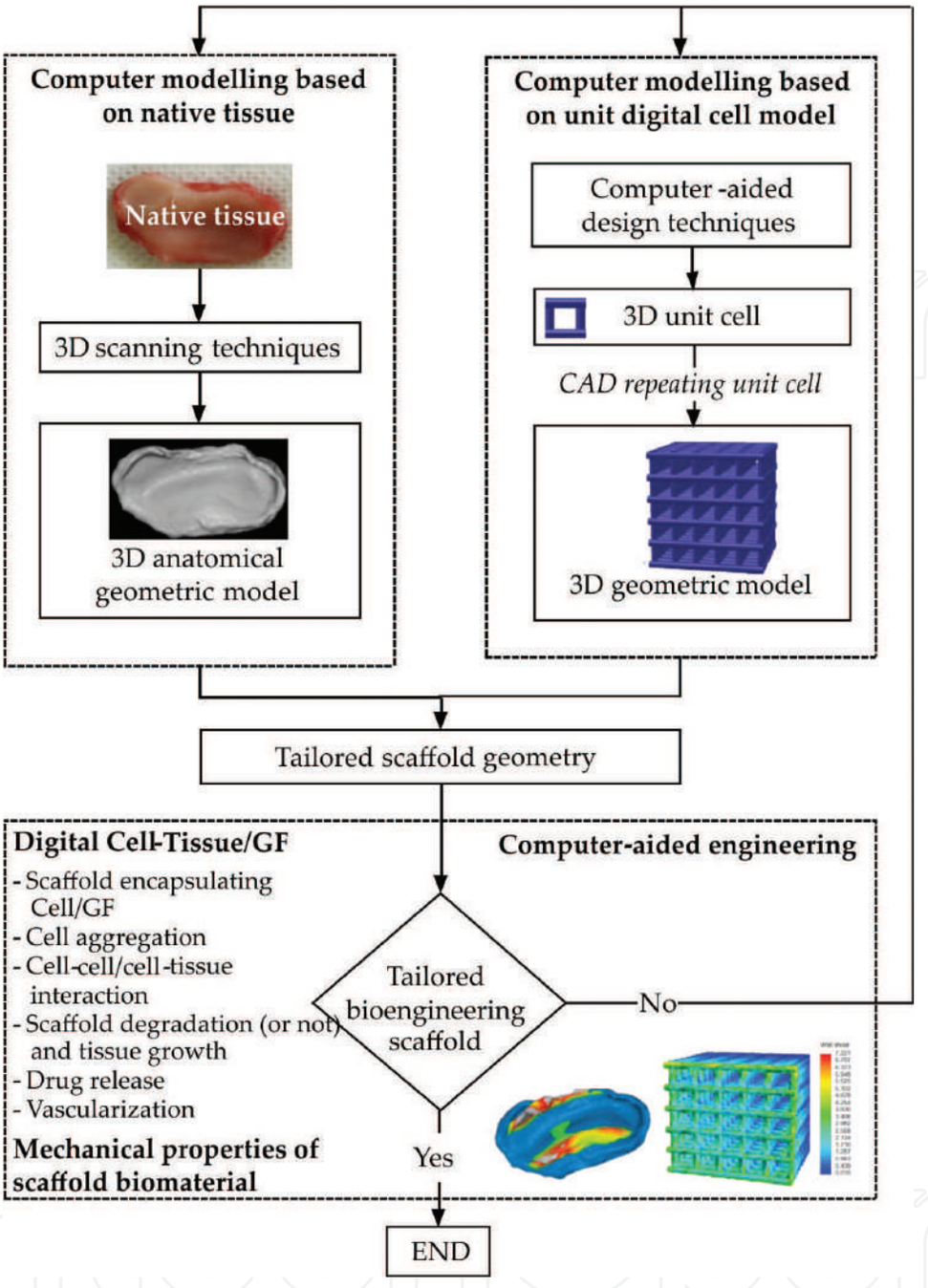

Figure 2. Computer modeling and simulation to tailor bioengineering scaffolds.

CT, these images are displayed by density, while in MRI they are compiled and segmented by its signal intensity. Additionally, both techniques can be differentiated by its resolution. The high resolution of CT allows the characterization of the micro-architecture and the mechanical properties of the tissue scaffolds [11]; however, this technique has a drawback regarding soft tissues of similar density. It is more efficient in differentiating hard tissues with sharply defined density changes, such as the interface between bone and soft tissues. To overcome this problem, contrast agents can be added [6]. Although the resolution of MRI is inferior to CT scans, with the advance of technology, it is improving, allowing the 3D representation of

internal structures, such as the central nervous system, heart, and kidneys of a rat [9]. The 2D individual images obtained using the previous techniques described are then assembled and realigned, and therefore a 3D geometric anatomical model distinguishing different types of tissue is obtained.

Microscopy optical technique is also used to obtain the 3D anatomical geometric model of the native tissue. However, it can only differentiate every type of tissue down to the level of the individual cell at the cost of a huge computational effort. Other 3D optical techniques, such as 3D structured light, cannot differentiate the types of tissues presented and only allow the generation of the outer 3D geometric model of the native sample. In the case of the native tissue sample (temporomandibular joint disc (TMJ disc)) presented in the flowchart of **Figure 2**, a 3D point cloud was obtained using a white light 3D scanning system (Steinbichler—COMET 5®), and then an appropriate software was applied to replicate the 3D geometric anatomical model of the TMJ disc [12].

Hybrid modalities can also be used to construct the 3D model of the same specimen in order to take the advantage of each technique to differentiate the different types of tissues [9].

The second approach uses computer-aided design (CAD) techniques to create a 3D unit cell which is used as pattern. Then, a desired number of patterns are automatically generated and combined until a complete 3D geometric model of the scaffold is obtained with controlled architecture (**Figure 2**). Following this approach, the main scientific achievements reported are based on permanent or temporary scaffolds.

Permanent tailored engineering scaffolds have been designed mainly for bone repair of large segmental defects caused by fracture, tumor, or infection. In 2013, Wieding et al. [13] reported a numerical study which is used to determine the suitability of open porous of titanium scaffolds to act as bone scaffolds under physiological loading conditions. Uniaxial compression structural modulus of the titanium scaffolds was tailored ranging from 3.5 to 19.1 GPa as a function of the scaffold porosity from 64 to 80%. Results revealed that minimizing the amount of material of the inner core had a smaller influence than increasing the porosity when the scaffolds were under biomechanical loading. It was also noted that the scaffold design could act similarly to the intact bone. In order to tailor the mechanical properties of cellular structured scaffolds, [14] designed metal scaffolds with high porosity (62–92%) to tailor both compressive strength (4.0–113.0 MPa) and elastic modulus (0.2–6.3 GPa), respectively, were comparable to trabecular and cortical bone. Porous titanium scaffolds were also investigated by van der Stok et al. [15, 16] for grafting large bone defects. Mechanical properties were tailored, whereas high porosity of the scaffold allowed the incorporation of colloidal gelatin gels for time- and dose-controlled delivery of dual growth factors (bone morphogenetic protein-2 (BMP-2) and/or fibroblast growth factor-2 (FGF-2)), promoting a quasi-full bone regeneration. The scaffold was designed based on a decahedron pattern and composed by 120-μm-thick titanium struts with porous size ranging from 240 to 730 μm. Porous size, porosity, porous volume, compression strength, and Young's modulus were 490 μm, 88%, 55 mm^3, 14 MPa, and 0.4 GPa, respectively, allowing to achieve an optimized bone volume regeneration (~50 mm^3) for a composite scaffold with BMP-2/FGF-2. In 2012, Van Bael et al. [17] developed six distinct geometries of Ti6Al4V scaffolds in three different pore shapes (triangular, hexagonal, and rectangular) and two different

pore sizes (500 and 1000 μm) aiming to understand the effect of pore geometry of Ti6Al4V bone scaffolds on the in vitro biological behavior of human periosteum-derived cells. The main result showed that a functional Ti6Al4V-graded scaffold, with specific morphological and mechanical properties, will contribute to enhance cell seeding and at the same time can maintain nutrient transport throughout the whole scaffold during in vitro culturing by avoiding pore occlusion.

Temporary (or biodegradable) tailored engineering scaffolds have been designed as a tissue engineering approach that uses degradable porous biomaterial incorporating biological cells and/or molecules to regenerate tissues such as the bone, cartilage, skeletal muscle, nerve, and blood vessels. Scaffold design must be able to create hierarchical porous structures to fulfill all mechanical and biological requirements. In 2005, Hollister [18] introduced the concept of hierarchical scaffold design as geometric features at scales from the nanometer to millimeter level that will determine how well the scaffold meets conflicting mechanical function and mass transport needs. In 2011, Khoda et al. [19] developed a functionally gradient variational porosity architecture (hierarchical design) for hollowed scaffolds. In 2014, Giannitelli et al. [20] reviewed tailored scaffold architecture with microstructural features. Authors highlighted the growing interest in the development of innovative scaffold designs to overcome often conflict requirements (such as biological and mechanical ones). Considering different pore size gradients, Sobral et al. [21] designed and manufactured. The goal was to enhance cell seeding efficiency and control the spatial organization of cells within the scaffold. Some authors [22] also emphasized the importance of scaffold pore size gradients in osteogenic differentiation of human mesenchymal stromal cells. In 2010, Puppi et al. [23] in deep reviewed the design of biodegradable and bioactive polymeric scaffolds, with properly suited architecture and tailored properties for bone and cartilage tissue regeneration. According to the authors, a good scaffold design must account that macro- and microstructural properties affect cells survival, signaling, growth, propagation, and reorganization and play also a major role in modeling cell shape and gene expressions, both related to cell growth and preservation of native phenotypes [24, 25]. In addition, several scaffold designs were developed and then manufactured using different AM processes. For example, Fierz et al. [26] designed three labeled anisotropic 3D hydroxyapatite scaffolds (pixel-wise and labeled layer-wise) with tailored pores ranging from the nanometer to millimeter scale for the reconstruction of centimeter-sized osseous defects. Seventy percent micrometer-wide pores were successfully interconnected, and virtual spheres (diameter of up to 350 ± 35 μm) were used to simulate cell migration along the pores linked with central channel. Melchels et al. [27] designed poly-DL-lactic acid (PDLLA) porous scaffolds with a gyroid architecture. This architecture was mathematically defined, allowing a precise control of porosity and pore size of a fully interconnected pore network. As noted by the authors, cell seeding of porous structures prepared from hydrophobic polymers, such as PDLLA, was difficult. Moreover, the penetration of a cell suspension was further hindered by the high tortuosity and poor interconnectivity of pore networks when manufactured by salt-leaching or freeze-drying conventional methods. Therefore, very open scaffold structure of the gyroid architecture that facilitates the penetration of water into PDLLA scaffold was manufactured by stereolithography. It was highlighted that the cells were well attached and homogeneously distributed throughout the porous scaffold. Good mechanical properties can be tailored in predesigned (porous) architectures from PDLLA based on gyroid architecture.

In 2012, Melchels et al. [28] reviewed additive manufacturing of tissues and organs. Authors also addressed tailored engineering scaffolds for breast reconstruction, focusing pore size and porosity for the generation of three scaffold models. Cipitria et al. [29] developed a poly (ε-caprolactone) (PCL) scaffold incorporating recombinant human bone morphogenetic protein 7 (rhBMP-7) for the regeneration of critical-sized defects in sheep tibiae. PCL scaffold with b-tricalcium phosphate (mPCL-TCP) to promote bone regeneration was designed based on a honeycomb structure with large interconnected pores to facilitate cellular bridging, ingrowth of bone tissue, and efficient mass transport and vascular infiltration. Moreover, Domingos et al. [30] developed PCL scaffolds for tissue engineering purposes. Authors addressed internal/external scaffold geometry, different material deposition strategies, and the biocompatibility of the material used. 3D PCL porous scaffolds (rectangular porous prisms) were designed with an average porosity of ~76% using commercial computer-aided design software. These structures were then produced via bioextrusion in a 0/90 lay-down pattern trying to reproduce a honeycomb-like pattern of fully interconnected square pores. Similar bioextruded scaffolds were designed (regular dimensions of 600 × 600 mm) to have a well-defined internal geometry with square interconnected pores and uniform distribution. The overall porosity of the structures was found to be ~76%. In vitro degradation of the scaffold was studied as a function of the degradation environment, pore size, and geometry [30, 31]. Scaffold degradation plays a key role when tailoring scaffold properties. In 2016, Morouço et al. [32] developed three types of PCL scaffolds reinforced with cellulose nanofibers (CNF), with and without the addition of hydroxyapatite nanoparticles (HANP), aiming to tailor scaffold properties for tissue engineering applications. The authors studied scaffold porosity, mechanical properties, and biocompatibility as a function of three material combinations. PCL, PCL/CNF, and PCL/CNF/HANP scaffolds were described with porous fully interconnected and porosity (%) of 49.0, 49.5, and 50.0; compressive modulus (MPa) of 54.42, 64.58, and 70.88; and maximum compressive stress (MPa) of 10.96, 11.35, and 12.12, respectively. These structures were then produced via bioextrusion in a 0/90 lay-down pattern. Some authors [33] studied hybrid hierarchical 3D scaffolds with well-controlled architecture for both macro- and microscale. Hybrid and hierarchical 3D structures include thick filaments with the diameter of hundreds of microns, and thin filaments with sub-10 μm dimensions were developed. The microscale features can help in cell seeding, alignment, and guidance. Trying to mimic morphological and mechanical behavior of a blood vessel, Vaz et al. [34] proposed a tailored tissue engineering scaffold. Design parameters such as bilayered tubular scaffold, stiff and oriented outside fibrous layer, and a pliable and randomly oriented fibrous inner layer were considered, combining two biomaterials (PLA/PCL). Structural and mechanical properties of the scaffolds were examined using scanning electron microscopy (SEM) and tensile testing. Cell viability was investigated using 3T3 mouse fibroblasts and the tubular scaffold in an appropriated in vitro environment. The proposed scaffold presented appropriate characteristics to be considered a candidate for blood vessel tissue engineering. Other authors also proposed to tailor tissue engineering scaffolds trying to mimic extracellular matrix morphology of natural tissue for blood vessel applications [35, 36].

In 2012, Chantarapanich et al. [37] developed a computer-aided design library based on polyhedrons for tissue engineering applications. Close-cellular scaffold included truncated octahedron, rhombicuboctahedron, and rhombitruncated cuboctahedron, while open-cellular

scaffold included hexahedron, truncated octahedron, truncated hexahedron, cuboctahedron, rhombicuboctahedron, and rhombitruncated cuboctahedron. Both relationship between pore size and porosity of close-cellular scaffolds and relationship between pore size/beam thickness and porosity of open-cellular scaffolds were studied. The study concluded that some design combinations were not good for making the open-cellular scaffold, generating enclosed pores inside the scaffold, and, therefore, they were excluded from the digital library. Compressive stresses were computed as a function of polyhedron-based geometries which can also be helpful for tailoring mechanical properties of the scaffolds.

In the computer-aided engineering based on tailored scaffold geometry, several digital features should be taken into account to obtain computer-tailored bioengineering scaffolds. Such features encompass cell and growth factor encapsulating, cell aggregation, cell-cell and cell-tissue interaction, vascularization, scaffold degradation (or not if permanent) and tissue growth, drug release, and scaffold mechanical behavior (**Figure 2**). To help digital prediction of cell/tissue phenomena, several automated methods exist, namely, cell counting, cell geometry determination, chromosomal counting, correlation of DNA expression determined through microarrays, interpreting fluorescence data, determining cell's lineage, and cross correlating gene expression with predicted in vivo pathology. All of these features have predictive value for determination of tissue viability and the differentiative rate of cells seeded with the goal of tissue culture. A detailed description about both accumulation of the expression data and large-scale computer cross correlation (between this expression and expressions commonly used in pathology) is provided in Ref. [9], as well as a number of specific tools for tissue analysis/identification.

Despite of the aforementioned research works, new scaffold designs integrating cell/GF/tissue phenomena and scaffold mechanical behavior (geometric characteristics and materials) are needed for regenerative medicine. These complex hierarchical 3D structures must be designed according to the structural heterogeneity of the host tissue and/or scaffold environment.

3. Biomaterials and scaffold bioactivity

Tissues possess different structures and properties that a tissue engineering scaffold should be tailored to. A general requirement for all biomaterial scaffolds is to reproduce an extracellular matrix (ECM) environment for supporting cell growth outside of the body. Moreover, scaffold should host cell adhesion, proliferation, and ECM production. Hence, the scaffold should surrogate the missing ECM. Tissue engineering products can be designed to conduct, induct, or block tissue responses and architectures [38]. Besides providing the three-dimensional growth of cells in an organized way, an ideal scaffold should be characterized by biocompatibility, biodegradability, appropriate mechanical properties, interconnectivity of pores with appropriate size to retain cells, and low exchanges of nutrients and waste products [39]. Tailoring biomaterials for enhanced biofunctionality can be achieved using a variety of approaches that involve the introduction of chemical, topographical, or mechanical cues via top-down or bottom-up approaches [40]. Therefore, the selection of the starting materials and of the fabrication techniques is of paramount importance. Numerous natural and

synthetic materials can be used for the fabrication of scaffolds including polymers, ceramics, bioactive glass, calcium phosphates, and biometals. For example, scaffolds fabricated from bioactive ceramic materials such as hydroxyapatite and tricalcium phosphate show promise because of their biological ability to support bone tissue regeneration. However, the use of ceramics as scaffold materials is limited because of their inherent brittleness and difficult processability [39]. In 2006, Rezwan et al.'s [41] review showed that conventional material processing methods have been adapted and extended for incorporation of inorganic bioactive phases into porous and interconnected 3D polymer networks. The biomaterials were extended from purely synthetic materials to material/biologic hybrids, engineering at the same time bioactivity and biodegradability [41]. Addressing this issues, in 2015, Fiedler et al. [42] focused on the mechanical characterization of PCL-bioglass composites and concluded that the addition of bioglass was found to decrease the elastic gradient and yield stress if two scaffolds of the same density are compared and the highest bioglass content (35%) seems beneficial as it (i) does not significantly deteriorate the scaffold mechanical properties and (ii) promotes bioactivity.

The next generation of synthetic biodegradable, bioactive, living composite biomaterials that feature high adaptiveness to the biological environment [41] considers the incorporation of biomolecules as promising and is currently under extensive research. Incorporating biomolecules such as growth factors during scaffold processing with the aim to accelerate local tissue healing however are not simple as biomolecules are sensitive to elevated temperatures and extreme chemical conditions. A promising strategy is the immobilization of proteins and growth factors in the post-processing phase via surface functionalization of the scaffold [43].

"Soft" material routes like sol-gel processing might be a strategy to incorporate biomolecules during scaffold fabrication. To the authors' knowledge, however, sol-gel-derived bioactive organic/inorganic hybrids have not yet been formed into highly interconnected porous structures, which would be essential for application of these composites as scaffolds. Another related challenge was the elucidation of the local impact of growth factors on the cell and tissue systems, including long-term effects [41]. As pointed out in Section 2, mechanical property is one of the most critical parameters that determine the performance of a designed implant. It mainly depends on the process and structural properties of the biomaterials. Therefore, it is possible to achieve desired mechanical properties through modifying the structural characteristics of a biomaterial. Biological behavior of cell assessment after surface modifications is required to check its biocompatibility and bioactivity [38]. The study of the interactions of biochemical and geometrical cues on stem cell differentiation and alignment should be also considered. The capability to spatially control stem cell orientation and differentiation toward multiple phenotypes simultaneously, i.e., myocyte, tenocyte, and osteoblast, allows cells grown in vitro to more closely mimic aspects of native tissue organization and structure [44]. Although the precise mechanism behind geometry-induced cell alignment is presently unknown, it is likely that the alignment of cells observed on fibers may be attributed to a combination of factors including physical space constraint and relative stiffness of the underlying substrate (fiber); ultimately affecting changes in both cell spreading and cell stiffness, cells may be predisposed toward a specific orientation through the modulation of mechanotransduction pathways via cytoskeletal rearrangements [9].

Multilayer scaffolds and combinations of several biomaterials are a better option to create graded structures that resemble the biological interface. The development of multilayer scaffolds and the controlled release of bioactive molecules to promote in situ regeneration of biological tissues are some of the latest technologies that intended to improve on the available traditional treatments. To confirm the potential of these novel approaches, long-term evaluation is necessary with special focus on studying the biological and mechanical properties of the synthesized tissues [45].

Scaffolds should be designed more as a bioactive system rather than just passive cell carriers. Thus, integration of fabrication techniques with surface modification may also act as route to obtain nanofibrous scaffolds with better understanding of cell scaffolds both in vivo and in vitro. Similarly and significantly, the biomaterial as design strategy can be used in a better way to relate science and engineering, and use this advanced knowledge to engineer more advanced tissue scaffolds [46, 47].

4. Biofabrication processes

Aiming to tailor bioengineering scaffolds that closely mimic the native tissues, AM technologies are suitable to dispense biomaterials (with live cells or cell aggregates) at specific, and desired, locations [48]. The usage of these technologies has been commonly divided in three categories: (i) the jet-based techniques, (ii) robotic dispensing techniques, and (iii) laser-induced forward transfer [49, 50]. Each of these techniques has advantages and drawbacks (**Table 1**). Thus, understanding its limitations and potentials is a must-do to choose the right approach for the specific tissue that is aimed to regenerate. Furthermore, some advancements have been recently achieved with integrated/hybrid systems. These systems combine different techniques within the same equipment aiming to generate a multifunctional graded construct with tailored properties similar to the native tissue.

In the available literature, it is possible to find investigations using different approaches, for the same type of tissue. In fact, there seems to be a trend to some research groups get specialized in some type of technology and use it for various goals.

	Jet based	**Robotic dispensing**	**Laser-induced forward transfer**
Resolution	+	+/–	++
Fabrication speed	+/–	++	–
Hydrogel viscosity	–	+	+/–
Gelation speed	++	+/–	++
Cell density	–	+	+/–

Adapted from Ref. [51].

Table 1. Comparison of the three AM approaches for tissue engineering.

Regarding the jet-based techniques, with a common resolution of 10–50 μm, it is difficult to obtain an adequate structural support. It consists of dispensing a jet of small droplets of liquid material, also called as bioink, in a spatially controlled manner. There are two different approaches, thermal inkjet printing and piezoelectric-actuated inkjet printing, having the former lower suitability for 3D bioengineering scaffolds. Using a piezoelectric actuator, research has been able to suppress some of the thermal constraints [51]. For instance, good viability of printed cell populations was obtained for human fibroblast cell line [52], and recently a silk-based ink eliminated the usage of any cytotoxic organic or inorganic solvents [53]. Even though jet-based techniques are the pioneer techniques used for tissue engineering, translating it to the construct of large 3D structures is a challenge to overcome, mostly because of the low-viscous solutions that do not provide strong and complex 3D structures.

The most successful attempts to engineer cell-containing bioengineering scaffolds have been achieved through robotic dispensing systems. These technologies are based on a controlled extrusion of a material in a continuous fashion, instead of liquid droplets (**Figure 3**) and are developed at the Center for Rapid and Sustainable Development (CDRSP) of the Polytechnic Institute of Leiria, Portugal. Therefore, this approach enables the printing of hydrogels encapsulating cells in a very controlled architecture [28]. The most common methods are the pneumatic [54] or mechanical [55] dispensing systems, comprising (i) a dispensing system and a stage with the capability of moving along the *x*, *y*, and *z* axes; (ii) a light source to illuminate the working area and/or for photoinitiator activation; and (iii) a piezoelectric humidifier [56], with some of them using multiple printing heads to permit the dispensing of various materials without retooling [57]. However, researcher should bear in mind that optimal balance should be aimed between pressure and nozzle size (to obtain higher cell viability).

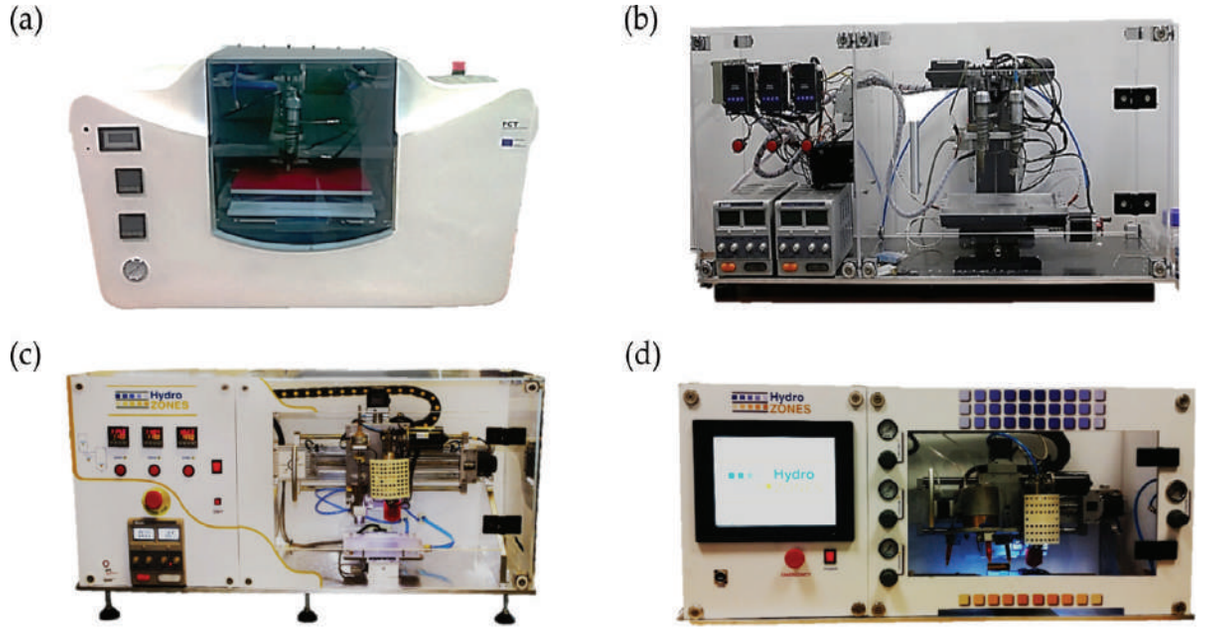

Figure 3. Equipments developed at the CDRSP, Portugal: (a) one-head extrusion system, (b) dual-head extrusion system, (c) system combining an extrusion head and a syringe for hydrogel deposition, and (d) hybrid system combining extrusion with up to three hydrogels.

Recently, a US research group presented an integrated tissue-organ printer (ITOP) for the production of human-scale tissue bioengineering scaffolds of any shape, in a single structure [50]. Combining different procedures, it was possible to successfully engineer (i) a mandible bone, (ii) an ear-shaped cartilage, and (iii) a skeletal muscle. Furthermore, some institutions are now combining different technologies, for instance, merging a robotic dispensing system with a jet-based printing for muscle-tendon unit repair [58].

Lastly, the laser-induced forward transfer (LIFT) is a not-so-common technology for tissue engineering, but is gaining significant importance in this domain [56]. It is based on using three layers of different components: the first layer based on a donor slide, covered by a laser energy-absorbing layer and completed with a cell-bioink component [51]. There are three main advantages for this technology: it is suitable for using (i) a wide range of materials, (ii) a very high precise deposition (but in small 3D structures), and (iii) a clog-free process without the use of nozzles. However, it requires a rapid gelation process, and researchers should bear in mind that several factors should be considered (e.g., laser wavelength, bioink viscosity; for more info read Ref. [59]). Apart from these constraints, successful cell viability (>90%) has been reported for printing skin cell lines and human mesenchymal stem cells and to prepare a cardiac patch [60].

5. Scaffold biodegradability and cell viability

The main objective of tissue engineering is to allow the cells of the body to replace the implanted scaffold over a period. Because bioengineering scaffolds are not intended as permanent implants (besides some of them have shown good results mainly in bone regeneration), they must therefore be biodegradable, so that the need of surgical removal can be avoided. Furthermore, the degradation products should be nontoxic and should be able to swiftly exit from the body without interference with other organs. In addition to this, the intermediate product, the timing of the degradation process, and the route and mechanism of degradation are equally important aspects that need to be taken care [47]. Scaffold materials should fulfill several requirements. A scaffold is not just a passive support for cell growth, but a device whose properties affects the regeneration cascade. Mechanical properties, surface properties, and morphology are in turn relevant to the specific application. Degradation kinetics and the rate at which scaffold properties change with degradation should always be predictable. In particular, the degradation behavior of biomaterials can follow several mechanisms and is controlled by different factors. Understanding the degradation kinetics and mechanism of biomaterials is necessary to optimize their possible usage. The rate of degradation is also strictly connected to the degree of porosity [38].

One of the general variables that need to be thoroughly considered to successfully bioprint viable and functional tissue bioengineering scaffolds is the inclusion of supportive biomaterials, generally in the form of proteins and polymers, which (1) facilitate the deposition method by mechanical means and (2) provide support and protection to the cells during and after the

tissue construct fabrication process. These biomaterials can encompass the physical environment inside of which the cells will reside, as well as the biochemical signal cells need to function as they would in the body [46].

Scaffolds represent the space available for the tissue to develop and the physical support for cell growth. Scaffold mechanical properties should allow shape maintenance during tissue regeneration and enable stress transfer and load bearing. Moreover, during the first stage of tissue reconstruction, wound contraction forces act against the process, and enough mechanical strength and stiffness of the scaffold is required. Scaffold porosity is a fundamental characteristic for providing available space for cells to migrate and for vascularization of the tissue. Furthermore, the larger the surface available, the more cell interactions will arise. In general, the biological activity of a scaffold is determined by ligand density. Scaffold composition and porous fraction, that is, the total surface of the structure exposed to cells, determine the ligand density. Highly specific surface areas allow for cell attachment and anchorage, and a high pore volume fraction enables cell growth, migration, and effective transportation of fluids and nutrients. In particular, microporosity is important for capillary ingrowth and interactions between cells and matrix, while macroporosity is relevant to nutrient supply and waste removal of cell metabolism. The rate of degradation is also strictly connected to the degree of porosity [38].

As in the development of the tissue-engineered organs, regeneration of functional tissue requires maintenance of cell viability and differentiated function, encouragement of cell proliferation, modulation of the direction and speed of cell migration, and regulation of cellular adhesion [61]. Cell viability may be judged by morphological changes or by changes in membrane permeability and/or physiological state inferred from the exclusion of certain dyes or the uptake and retention of others. Cultured cells are seeded onto a three-dimensional biocompatible scaffold that will slowly degrade and resorb as the soft and hard structures grow and assimilate in vitro and/or in vivo [2]. Cell viability during 3D bioprinting is dependent on the shear stress experienced during extrusion, which in turn is dependent on the viscosity of the solution, the applied pressure, and the needle diameter. In addition, any post-printing bioink cross-linking may also impact on cell viability [62]. Cell viability can be measured with Live/Dead Viability/Cytotoxicity assay after printing [63] and could vary with dispensing pressure and nozzle diameter. It decreases as the pressure increases and the nozzle diameter decreases, and it is seen that the effect of pressure is significantly larger than the effect of the nozzle diameter. At higher pressures, there is an increase in the number of apoptotic cells as well as necrotic cells [64].

Tissue bioengineered scaffolds targeted for in vivo applications are typically restricted to a thickness of only a few hundreds of microns, owing to the diffusion limitations of oxygen and nutrients [43]. One of the major challenges in tissue engineering for translation in clinical applications is the vascularization of bioengineering scaffolds of clinically relevant size. Insufficient vascularization inhibits nutrient and host cell delivery or migrations and leads to improper cell integration or cell death. While vascularization remains a challenge to maintain viability of large biofabricated tissue bioengineering scaffolds, recent advances in the field demonstrate that novel biofabrication techniques may resolve this problem [65].

6. New insights: 3D to 4D

Doing a survey on the Web of Science®, it is noticeable that the number of original articles on tissue engineering and regenerative medicine has experienced a tremendous increase over the past 10 years (**Figure 4**; review papers and proceedings not included). Likewise, bioprinting is attracting a lot of researchers presenting an exponential increase in the last 3 years. Meanwhile, 3D bioprinting market was valued at $98.6 million in 2015, and an annual growth of 36% for the next 6 years is expected [66].

Nevertheless, 3D bioprinting has been focused on the development of bioengineering scaffolds that lack a crucial element for mimicking native live tissues: its ability to acutely change according to its function. That is why leading research groups have recently proposed the four-dimensional (4D) bioprinting (time is integrated with 3D bioprinting) as an enhanced approach for tissue engineering and regenerative medicine: the development of stimuli-responsive biomaterials that can be printed and dynamic to intended stimulation. However, several challenges arise, namely, (i) bioinks have to be optimized to achieve successful bioprinting; (ii) processes must be mechanically designed to obtain robust shape-changing capability of the bioengineering scaffolds [67]; (iii) specific bioreactors for complex tissue function maturation need to be invented; and (iv) evaluation procedures should be defined to examine the functionality response.

Therefore, the most promising approach is to optimize the cell-bioengineering scaffold interactions, becoming feasible to explore the usage of computer modeling to examine the further responses. Developing "smart" biomaterials (also referred as "intelligent," "stimuli responsive," "stimuli sensitive," or "environmentally sensitive") to allow the dynamic changes of the structure, upgrade of the printing processes into defined architecture for targeting tissues,

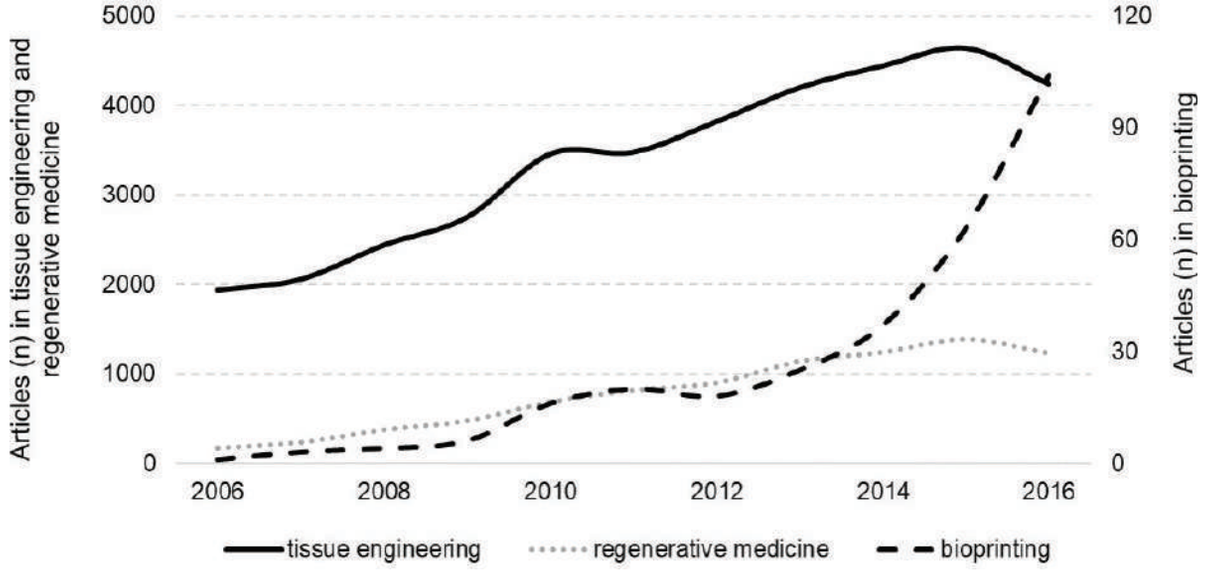

Figure 4. Number of original articles on tissue engineering and regenerative medicine 2006–2016.

automation of stimulus, and standardizing the assessment procedures to evaluate the result is crucial for enhanced regenerative medicine approaches [68].

Acknowledgements

This publication is supported by the Portuguese Foundation for Science and Technology (FCT) through the following projects: UID/Multi/04044/2013 and PTDC/EMS-SIS/7032/2014.

Author details

Sandra Amado[1,2,3]*, Pedro Morouço[1], Paula Pascoal-Faria[4] and Nuno Alves[1,5]

*Address all correspondence to: sandra.amado@ipleiria.pt

1 Centre for Rapid and Sustainable Product Development, Polytechnic Institute of Leiria, Leiria, Portugal

2 CIPER-FMH, Centro Interdisciplinar de Estudo de Performance Humana, Faculdade de Motricidade Humana (FMH), Universidade de Lisboa (UL), Lisboa, Portugal

3 School of Health Sciences at the Polytechnic Institute of Leiria, Leiria, Portugal

4 Centre for Rapid and Sustainable Product Development & Mathematics Department, School of Technology and Management, Polytechnic Institute of Leiria, Leiria, Portugal

5 Mechanical Engineering Department, School of Technology and Management, Polytechnic Institute of Leiria, Leiria, Portugal

References

[1] Morouço P, Alves N, Amado S. The role of biomechanics in tissue engineering. Austin Journal of Biomedical Engineering. 2016;**3**(1):1-2

[2] Hutmacher DW. Scaffold design and fabrication technologies for engineering tissues—state of the art and future perspectives. Journal of Biomaterials Science Polymer Edition. 2001;**12**(1):107-124

[3] Malda J, Groll J. A step towards clinical translation of biofabrication. Trends in Biotechnology. 2016;**34**(5):356-357

[4] Zadpoor AA, Malda J. Additive manufacturing of biomaterials, tissues, and organs. Annals of Biomedical Engineering. 2017;**45**(1):1-11

[5] Parker GJM, Wheeler-Kingshott CAM, Barker GJ. Diffusion tensor imaging. IEEE Transactions on Medical Imaging. 2002;**21**(5):505-512

[6] Fang Z, Starly B, Sun W. Computer-aided characterization for effective mechanical properties of porous tissue scaffolds. CAD Computer-Aided Design. 2005;**37**(1):65-72

[7] Zadpoor A.A.. Bone tissue regeneration: The role of scaffold geometry. Biomaterials Science. 2015;**3**(2):231-245

[8] Folch A, Mezzour S, Düring M, Hurtado O, Toner M, Müller R. Stacks of microfabricated structures as scaffolds for cell culture and tissue engineering. Biomedical Microdevices. 2000;**2**(3):207-214

[9] Sun W, Darling A, Starly B, Nam J. Computer-aided tissue engineering: Overview, scope and challenges. Biotechnology and Applied Biochemistry. 2004;**39**(Pt 1):29-47

[10] Landers R, Hubner U, Schmelzeisen R, Mulhaupt R. Rapid prototyping of scaffolds derived from thermoreversible hydrogels and tailored for applications in tissue engineering. Biomaterials. 2002;**23**(23):4437-4447

[11] Lin A, Barrows T, Cartmell S, Guldberg R. Microarchitectural and mechanical characterization of oriented porous polymer scaffolds. Biomaterials. 2003;**24**(3):481-489

[12] Angelo DF, Morouço P, Alves N, Viana T, Santos F, González R, et al. Choosing sheep (*Ovis aries*) as animal model for temporomandibular joint research: Morphological, histological and biomechanical characterization of the joint disc. Morphologie. 2016; **100**(331):223-233

[13] Wieding J, Souffrant R, Mittelmeier W, Bader R. Finite element analysis on the biomechanical stability of open porous titanium scaffolds for large segmental bone defects under physiological load conditions. Medical Engineering and Physics. 2013;**35**(4):422-432

[14] Cheng XY, Li SJ, Murr LE, Zhang ZB, Hao YL, Yang R, et al. Compression deformation behavior of Ti-6Al-4V alloy with cellular structures fabricated by electron beam melting. Journal of the Mechanical Behavior of Biomedical Materials. 2012;**16**(1):153-162

[15] Van Der Stok J, Koolen MKE, De Maat MPM, Amin Yavari S, Alblas J, Patka P, et al. Full regeneration of segmental bone defects using porous titanium implants loaded with BMP-2 containing fibrin gels. European Cells & Materials. 2015;**29**:141-154

[16] van der Stok J, Wang H, Amin Yavari S, Siebelt M, Sandker M, Waarsing JH, et al. Enhanced bone regeneration of cortical segmental bone defects using porous titanium scaffolds incorporated with colloidal gelatin gels for time- and dose-controlled delivery of dual growth factors. Tissue Engineering Part A. 2013;**19**(23-24):2605-2614

[17] Van Bael S, Chai YC, Truscello S, Moesen M, Kerckhofs G, Van Oosterwyck H, et al. The effect of pore geometry on the in vitro biological behavior of human periosteum-derived cells seeded on selective laser-melted Ti6Al4V bone scaffolds. Acta Biomaterialia. 2012;**8**(7):2824-2834

[18] Hollister SJ. Porous scaffold design for tissue engineering. Nature Materials. 2005 Jul;**4**(7):518-524

[19] Khoda KM, Ozbolat IT, Koc B. A functionally gradient variational porosity architecture for hollowed scaffolds fabrication. Biofabrication. 2011;**3**(3):34106

[20] Giannitelli S, Mozetic P, Trombetta M, Rainer A. Combined additive manufacturing approaches in tissue engineering. Acta Biomaterialia. 2015;**24**:1-11

[21] Sobral JM, Caridade SG, Sousa RA, Mano JF, Reis RL. Three-dimensional plotted scaffolds with controlled pore size gradients: Effect of scaffold geometry on mechanical performance and cell seeding efficiency. Acta Biomaterialia. 2011;**7**(3):1009-1018

[22] Di Luca A, Szlazak K, Lorenzo-Moldero I, Ghebes CA, Lepedda A, Swieszkowski W, et al. Influencing chondrogenic differentiation of human mesenchymal stromal cells in scaffolds displaying a structural gradient in pore size. Acta Biomaterialia. 2016;**36**(March):210-219

[23] Puppi D, Chiellini F, Piras MM, Chiellini E. Polymeric materials for bone and cartilage repair. Progress in Polymer Science. 2010;**35**(4):403-440

[24] Chua C, Leong K, Lim C. Classification of rapid prototyping systems. In: Chua C, Leong K, Lim C, editors. Rapid Prototyping: Principles and Applications. Singapore: World Scientific Publishing; 2003. pp. 19-23

[25] Karageorgiou V, Kaplan D. Porosity of 3D biomaterial scaffolds and osteogenesis. Biomaterials. 2005;**26**:5474-5491

[26] Fierz FC, Beckmann F, Huser M, Irsen SH, Leukers B, Witte F, et al. The morphology of anisotropic 3D-printed hydroxyapatite scaffolds. Biomaterials. 2008;**29**(28):3799-3806

[27] Melchels FPW, Feijen J, Grijpma DW. A poly(d,l-lactide) resin for the preparation of tissue engineering scaffolds by stereolithography. Biomaterials. 2009;**30**(23-24):3801-3809

[28] Melchels FPW, Domingos MAN, Klein TJ, Malda J, Bartolo PJ, Hutmacher DW. Additive manufacturing of tissues and organs. Progress in Polymer Science. 2012;**37**(8):1079-1104

[29] Cipitria A, Reichert JC, Epari DR, Saifzadeh S, Berner A, Schell H, et al. Polycaprolactone scaffold and reduced rhBMP-7 dose for the regeneration of critical-sized defects in sheep tibiae. Biomaterials. 2013;**34**(38):9960-9968

[30] Domingos M, Dinucci D, Cometa S, Alderighi M, Bártolo PJ, Chiellini F. Polycaprolactone scaffolds fabricated via bioextrusion for tissue engineering applications. International Journal of Biomaterials. 2009;**2009**:239643

[31] Domingos M, Chiellini F, Cometa S, De Giglio E, Grillo-Fernandes E, Bártolo P, et al. Evaluation of in vitro degradation of PCL scaffolds fabricated via BioExtrusion. Part 1: Influence of the degradation environment. Virtual and Physical Prototyping. 2010;**5**(2):65-73. Available from: http://www.tandfonline.com/doi/abs/10.1080/17452751003769440

[32] Morouço P, Biscaia S, Viana T, Franco M, Malça C, Mateus A, et al. Fabrication of poly(ε-caprolactone) scaffolds reinforced with cellulose nanofibers, with and without the addition of hydroxyapatite nanoparticles. BioMed Research International. 2016;**2016**:1-10

[33] Wei C, Dong J. Hybrid hierarchical fabrication of three-dimensional scaffolds. Journal of Manufacturing Processes. 2014;**16**(2):257-263

[34] Vaz CM, van Tuijl S, Bouten CVC, Baaijens FPT. Design of scaffolds for blood vessel tissue engineering using a multi-layering electrospinning technique. Acta Biomaterialia. 2005;**1**(5):575-582

[35] Nemeno-Guanzon JG, Lee S, Berg JR, Jo YH, Yeo JE, Nam BM, et al. Trends in tissue engineering for blood vessels. Journal of Biomedicine and Biotechnology. 2012;**2012**

[36] Hoenig MR, Campbell GR, Rolfe BE, Campbell JH. Tissue-engineered blood vessels: Alternative to autologous grafts? Arteriosclerosis, Thrombosis, and Vascular Biology. 2005;**25**(6):1128-1134

[37] Chantarapanich N, Puttawibul P, Sucharitpwatskul S, Jeamwatthanachai P, Inglam S, Sitthiseripratip K. Scaffold library for tissue engineering: A geometric evaluation. Computational and Mathematical Methods in Medicine. 2012;**2012**

[38] Haycock J. 3D Cell Culture [Internet]. Vol. 695, Image (Rochester, N.Y.). 2011. pp. 261-280

[39] Seol YJ, Park DY, Park JY, Kim SW, Park SJ, Cho DW. A new method of fabricating robust freeform 3D ceramic scaffolds for bone tissue regeneration. Biotechnology and Bioengineering. 2013;**110**(5):1444-1455

[40] Camarero-Espinosa S, Cooper-White J. Tailoring biomaterial scaffolds for osteochondral repair. International Journal of Pharmaceutics. 2016;**523**(2): 476-489

[41] Rezwan K, Chen QZ, Blaker JJ, Boccaccini AR. Biodegradable and bioactive porous polymer/inorganic composite scaffolds for bone tissue engineering. Biomaterials. 2006;**27**(18):3413-3431

[42] Fiedler T, Videira AC, Bártolo P, Strauch M, Murch GE, Ferreira JMF. On the mechanical properties of PLC-bioactive glass scaffolds fabricated via BioExtrusion. Materials Science and Engineering C. 2015;**57**:288-293

[43] Cosson S, Otte EA, Hezaveh H, Cooper-White JJ. Concise review: Tailoring bioengineered scaffolds for stem cell applications in tissue engineering and regenerative medicine. Stem Cells Translational Medicine. 2015;**4**(2):156-164

[44] Ker EDF, Nain AS, Weiss LE, Wang J, Suhan J, Amon CH, et al. Bioprinting of growth factors onto aligned sub-micron fibrous scaffolds for simultaneous control of cell differentiation and alignment. Biomaterials. 2011;**32**(32):8097-8107

[45] López-Ruiz E, Jiménez G, García MÁ, Antich C, Boulaiz H, Marchal JA, et al. Polymers, scaffolds and bioactive molecules with therapeutic properties in osteochondral pathologies: What's new? Expert Opinion on Therapeutic Patents. 2016;**26**(8):877-890

[46] Cheung DYC, Duan B, Butcher JT. Essentials of 3D Biofabrication and Translation [Internet]. Essentials of 3D Biofabrication and Translation. 2015. pp. 351-370

[47] Kariduraganavar MY. Advances in polymers and tissue engineering scaffolds. In: Inamuddin, editor. Green Polymer Composites Technology Properties and Applications. Boca Raton: Taylor & Francis Group; 2016;343-354

[48] Gao B, Yang Q, Zhao X, Jin G, Ma Y, Xu F. 4D bioprinting for biomedical applications. Trends in Biotechnology. 2016;**34**(9):746-756

[49] Melchels F, Malda J, Fedorovich N, Alblas J, Woodfield T. Organ Printing; Comprehension Biomaterials; 2011;**5**:587-606

[50] Kang H-W, Lee SJ, Ko IK, Kengla C, Yoo JJ, Atala A. A 3D bioprinting system to produce human-scale tissue constructs with structural integrity. Nature Biotechnology. 2016;**34**(3):312-319

[51] Malda J, Visser J, Melchels F, JÜngst T, Hennink W, Dhert W, et al. 25th anniversary article: Engineering hydrogels for biofabrication. Advanced Materials. 2013;**25**:5011-5028

[52] Saunders R, Gough J, Derby B. Delivery of human fibroblast cells by piezoelectric drop-on-demand inkjet printing. Biomaterials. 2008;**29**:193-203

[53] Tao H, Marelli B, Yang M, An B, Onses M, Rogers J, et al. Inkjet printing of regenerated silk fibroin: From printable forms to printable functions. Advanced Materials. 2015;**27**:4273-4279

[54] Chang C, Boland E, Williams S, Hoying J. Direct- write bioprinting three-dimensional biohybrid systems for future regenerative therapies. Journal of Biomedical Materials Research. Part B, Applied Biomaterials. 2011;**98**:160-170

[55] Visser J, Peters B, Burger T, Boomstra J, Dhert W, Melchels F, et al. Biofabrication of multi-material anatomically shaped tissue constructs. Biofabrication. 2013;**5**(3):35007

[56] Murphy S, Atala A. 3D bioprinting of tissues and organs. Nature Biotechnology. 2014; Aug;**32**(8):773-785

[57] Mironov V, Visconti R, Kasyanov V, Forgacs G, Drake C, Markwald R. Organ printing: Tissue spheroids as building blocks. Biomaterials 2009;**30**:2164-2174

[58] Merceron T, Burt M, Seol Y, Kang H, Lee S, Yoo J, et al. A 3D bioprinted complex structure for engineering the muscle-tendon unit. Biofabrication. 2015;**7**:35003

[59] Guillemot F, Souquet A, Catros S, Guillotin B. Laser- assisted cell printing: Principle, physical parameters versus cell fate and perspectives in tissue engineering. Nanomedicine. 2010;**5**:507-515

[60] Gaebel R, Ma N, Liu J, Guan J, Koch L, Klopsch C, et al. Patterning human stem cells and endothelial cells with laser printing for cardiac regeneration. Biomaterials. 2011;**32**:9218-9230

[61] Khang G. Handbook of Intelligent Scaffolds for Tissue Engineering and Regenerative Medicine; Singapore: Taylor & Francis Group; 2012. 1-972 pp

[62] Daly AC, Critchley SE, Rencsok EM, Kelly DJ. A comparison of different bioinks for 3D bioprinting of fibrocartilage and hyaline cartilage. Biofabrication. 2016;**8**(4):45002

[63] Cui X, Breitenkamp K, Finn MG, Lotz M, D'lima DD. Direct human cartilage repair using three-dimensional bioprinting technology. Tissue Engineering Part A. 2012;**18**:1304-1312

[64] Nair K, Gandhi M, Khalil S, Yan KC, Marcolongo M, Barbee K, et al. Characterization of cell viability during bioprinting processes. Biotechnology Journal. 2009;**4**(8):1168-1177

[65] Lim K, Morouço P, Levato R, Melchels F, Malda J. Organ Biofabrication. Comprehension Biomaterials II; 2017;**5**:236-266

[66] Market Research P&S. Global 3D Bioprinting Market Size, Share, Development, Growth and Demand Forecast to 2022, 2016. Available from (https://www.psmarketresearch.com/press-release/3d-bioprinting-market)

[67] Li Y-C, Zhang YS, Akpek A, Shin SR, Khademhosseini A. 4D bioprinting: The next-generation technology for biofabrication enabled by stimuli-responsive materials. Biofabrication. 2016 2;**9**(1):012001

[68] Furth ME, Atala A, Van Dyke ME. Smart biomaterials design for tissue engineering and regenerative medicine. Biomaterials. 2007;**28**(34):5068-5073